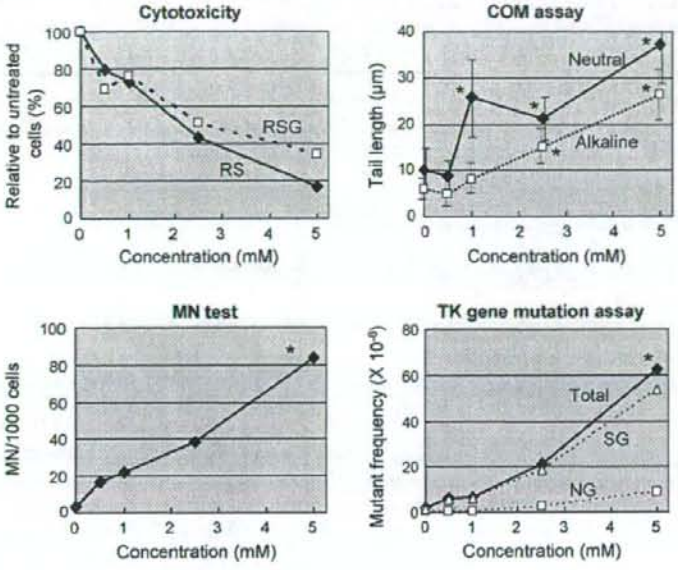

Fig. 1. Cytotoxic (relative survival, RS; relative suspension growth, RSG) and genotoxic responses (COM assay, MN test, and *TK* gene mutation assay) of TK6 cells treated with $KBrO_3$ for 4 h. Asterisk (*) statistically significant in Dunnett's test ($P < 0.05$) in COM assay, and in both pair-wise comparison and trend test ($P < 0.05$) in MN test and *TK* gene mutation assay.

mutations. Table 1 also shows the results of LOH analysis of the induced and spontaneously occurring mutants. The result of molecular analysis of spontaneous *TK* mutants was reported previously [21]. We classified the mutants into three types: non-LOH, hemizygous LOH (hemi-LOH), and homozygous LOH (homo-LOH). In general, hemi-LOH is resulted by deletion and homo-LOH is by inter-allelic homologous recombination [20]. Among the $KBrO_3$-induced mutants, 63% of NG mutants and 84% of SG mutants were hemi-LOH. In spontaneous mutants, on the other hand, majority of NG and SG mutants were non-LOH and homo-LOH, respectively. These results indicated that $KBrO_3$ predominantly induced large deletions. We previously reported the mutational spectra of *TK* mutants in TK6 cells that treated with the alkylating agent ethylmethane sulfonate (EMS), or X-irradiated [20,21]. Fig. 2 shows the comparison of the mutational spectra of spontaneous and induced *TK* mutants by EMS, X-irradiation, and $KBrO_3$. The mutation spectrum induced by $KBrO_3$ was similar to that induced by X-radiation (which also induces LOH, predominantly via deletion [21]) but not by EMS. The majority of the mutations induced by $KBrO_3$ were large deletions, but not point mutations.

Fig. 3 shows the regions of LOH and the distribution of spontaneous, X-ray-induced, and $KBrO_3$-induced

Table 1
Cytotoxic and mutational responses to $KBrO_3$, and the results of LOH analysis of normally growing (NG) and slowly growing (SG) *TK* mutants

Treatment	Cytotoxic and mutational response			LOH analysis at *TK* gene (%)			
	RSG (%)	MF ($\times 10^{-6}$)	% SG	Number	Non-LOH	Hemi-LOH	Homo-LOH
Spontaneous[a]	100	2.19	56	56			
NG mutants				19	14 (74)	3 (16)	2 (11)
SG mutants				37	0 (0)	9 (24)	28 (76)
$KBrO_3$ (2.5 mM)	51	29.4	74	39			
NG mutants				8	3 (37)	5 (63)	0 (0)
SG mutants				31	1 (3)	27 (84)	4 (13)

[a] Data from Zhan et al. [22].

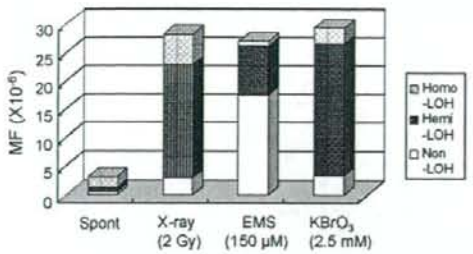

Fig. 2. *TK* mutation spectra in untreated, X-ray-treated (2 Gy), EMS-treated (150 μM, 4 h), and $KBrO_3$-treated (2.5 mM, 4 h) TK6 cells. The fraction of each mutational event was calculated by considering the ratio of NG to SG mutants and the results of molecular analysis (Table 1). The data for all but the $KBrO_3$ treatments were taken from our previous paper [20].

LOH mutants. $KBrO_3$ predominantly induced hemi-LOH, the result of large interstitial and terminal deletions, which we also frequently observed in the X-ray-induced LOH mutants. These results indicate that the genetic changes induced by $KBrO_3$ were similar to those induced by X-rays.

3.3. Gene expression analysis

Table 2 lists the genes that significantly increased expression following exposure to 2.5 mM $KBrO_3$. These genes are involved in stress response (6 genes), cell growth and DNA repair (19 genes), immune response (3 genes), apoptosis (3 genes), signal transduction (10 genes), transcription regulation (10 genes), chromosome organization (2 genes), protein modification (7 genes), energy metabolism (6 genes), lipid metabolism (2 genes), purine biosynthesis (3 genes), and unclassified functions (42 genes). Table 3 shows the genes whose expression was suppressed by the treatment. The number of up-regulated genes was greater that the number of down-regulated genes.

4. Discussion

$KBrO_3$ is a complete carcinogen, possessing both initiating and promoting activities in rodents [1]. While it shows clear positive responses in the COM assay, MN test, and chromosome aberration test using mammalian cells [4,14,17], the mutagenic potential of $KBrO_3$ in bacteria and the *Hprt* assay in Chinese hamster cells is weak or negative [1,14,17,30]. In our present study, $KBrO_3$ treatment strongly induced *TK* gene mutations. The reason we observed the induction of gene mutations and others did not is that $KBrO_3$ induces detectable mutagenecity in the *TK* gene but are only weakly mutagenic or non-mutagenic in the *Hprt* gene and in microbial assays [20]. The lower mutation frequency in the *Hprt* gene is due to the low recovery of large deletions, which are not detected because they are lethal. $KBrO_3$ is positive in mouse lymphoma cell assays that target the *Tk* gene [5]. In in vivo genotoxicity tests, $KBrO_3$ strongly induces MN in male ddY mice but is only weakly mutagenic in the *gpt* mutation assay in transgenic mice, which mainly detects point mutations and small deletions [31]. These results indicate that the property of genotoxicity

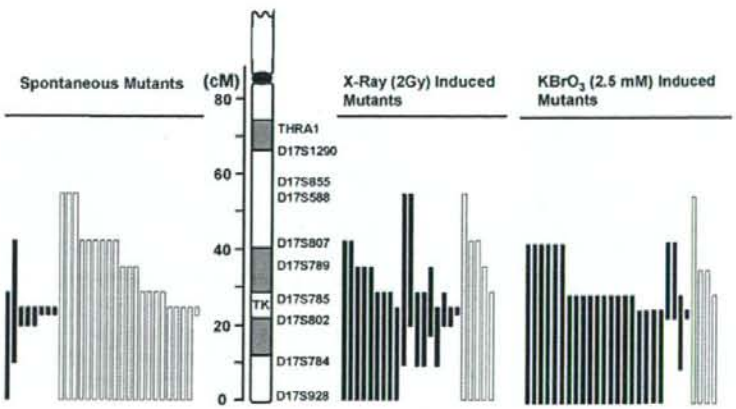

Fig. 3. The extent of LOH at the *TK* locus of TK6 cells that were untreated, X-ray-irradiated (2 Gy), or exposed to $KBrO_3$ (2.5 mM, 4 h). We examined 10 microsatellite loci on chromosome 17q that are heterozygous in TK6 cells. The human *TK* locus maps to 17q23.2. Open and closed bars represent homozygous LOH and hemizygous LOH, respectively. The length of the bar indicates the extent of the LOH. We analyzed 28 LOH mutants (4 NG and 24 SG). The data on spontaneous and X-ray-induced mutants were taken from our previous paper [20].

Table 2
Genes whose expression was up-regulated by $KBrO_3$ (2.5 mM, 4 h)

	Gene symbol	Ratio	Gene title
Stress response	CAT	2.77	Catalase
	DNAJC7	2.33	DnaJ (Hsp40) homolog, subfamily C, member 7
	FKBP5	2.87	FK506 binding protein 5
	HSPA8	3.02	Heat shock 70 kDa protein 8
	HSPCB	3.21	Heat shock 90 kDa protein 1, beta
	HSPD1	1.83	Heat shock 60 kDa protein 1
DNA repair, cell cycle, cell growth	BUB1	4.51	BUB1 budding uninhibited by benzimidazoles 1 homolog
	CCND2	5.08	Cyclin d2
	CCT2	3.33	Chaperonin containing TCP1, subunit 2 (beta)
	DKC1	2.37	Dyskeratosis congenita 1, dyskerin
	ENO1	2.10	Enolase 1 (alpha)
	HMGB1	2.16	High-mobility group box 1
	MAPRE1	2.32	Microtubule-associated protein, RP/EB family, member 1
	NME1	2.00	Non-metastatic cells 1, protein (NM23A) expressed in
	NOLC1	2.99	Nucleolar and coiled-body phosphoprotein 1
	NRAS	2.54	Neuroblastoma RAS viral (v-ras) oncogene homolog
	p21	3.22	Cyclin-dependent kinase inhibitor 1A (p21, Cip1)
	PPP2R1B	2.45	Protein phosphatase 2 (formerly 2A), regulatory subunit A (PR 65), beta isoform
	RAD21	2 34	RAD21 homolog
	RBBP4	2.00	Retinoblastoma binding protein 4
	RHOA	1.77	ras homolog gene family, member A
	SRPK1	2.75	SFRS protein kinase 1
	SSR1	2.66	Signal sequence receptor, alpha
Immune response	ARHGDIB	1.78	Rho GDP dissociation inhibitor (GDI) beta
	HLA-DRA	2.16	Major histocompatibility complex, class II, DR alpha
	IL2RG	2.43	Interleukin 2 receptor, gamma
Apoptosis	BCLAF1	6.42	BCL2-associated transcription factor 1
	FXR1	3.32	Fragile X mental retardation, autosomal homolog 1
	VDAC1	1.94	Voltage-dependent anion channel 1
Signal transduction	ANP32A	3.20	Acidic (leucine-rich) nuclear phosphoprotein 32 family, member A
	OGT	2.74	O-linked *N*-acetylglucosamine (GlcNAc) transferase
	PIP5K1A	4.25	Phosphatidylinositol-4-phosphate 5-kinase, type I, alpha
	PLEK	2.95	Pleckstrin
	PTPN11	2.61	Protein tyrosine phosphatase, non-receptor type 11
	SPTLC1	2.62	Serine palmitoyltransferase, long chain base subunit 1
	SRPR	2.52	Signal recognition particle receptor
Transcription regulation	CDC5L	4.37	CDC5 cell division cycle 5-like
	HNRPC	4.40	Heterogeneous nuclear ribonucleoprotein C (C1/C2)
	MED6	2.45	Mediator of RNA polymerase II transcription, subunit 6 homolog
	MED6	2.45	Mediator of RNA polymerase II transcription, subunit 6 homolog
	NO NO	2.68	Non-POU domain containing, octamer-binding
	POLR1C	2.67	Polymerase (RNA) I polypeptide C, 30 kDa
	PRPF4	2.51	PRP4 pre-mRNA processing factor 4 homolog
Chromosome organization	CBX5	2.68	Chromobox homolog 5 (HP1 alpha homolog, Drosophila)
Protein modification	CANX	2.56	Calnexin
	COPA	6.55	Coatomer protein complex, subunit alpha
	EIF2S3	2.40	Eukaryotic translation initiation factor 2, subunit 3 gamma
	EIF4B	2.86	Eukaryotic translation initiation factor 4B
	RANBP2	3.96	RAN binding protein 2
	SEC23IP	2.67	SEC23 interacting protein

Table 2 (*Continued*)

	Gene symbol	Ratio	Gene title
Energy pathway	AFURS1	2.83	ATPase family homolog up-regulated in senescence cells
	CYB5-M	2.54	Cytochrome *b*5 outer mitochondrial membrane precursor
	TOMM22	3.07	Translocase of outer mitochondrial membrane 22 homolog
Lipid metabolism	HMGCS1	2.58	3-Hydroxy-3-methylglutaryl-Coenzyme A synthase 1
	SCD	2.56	Stearovl-CoA desaturase
Purine biosynthesis	ENTPD1	2.36	Ectonucleoside triphosphate diphosphohydrolase 1
	GART	2.64	Phosphoribosylglycinamide formyltransferase
	PAICS	1.79	Phosphoribosylaminoimidazole carboxylase
Unclassified	BANF1	2.77	Barrier to autointegration factor 1
	BAT1	1.95	HLA-B associated transcript 1///HLA-B associated transcript 1
	C1orf16	2.37	Chromosome 1 open reading frame 16
	CALU	2.40	Calumenin
	DAZAP2	2.57	DAZ associated protein 2
	DDX18	2.34	DEAD (Asp-Glu-Ala-Asp) box polypeptide 18
	DHX9	9.37	DEAH (Asp-Glu-Ala-His) box polypeptide 9
	EXOSC2	3.03	Exosome component 2
	FLJ10534	2.07	Hypothetical protein FLJ10534
	FLJ10719	2.42	Hypothetical protein FLJ10719
	FLJ12973	2.76	Hypothetical protein FLJ12973
	GANAB	2.07	Glucosidase, alpha; neutral AB
	HEM1	2.37	Hematopoietic protein 1
	IGHM	2.76	Anti-HIV-1 gp120 V3 loop antibody DO142-10 light chain variable region
	IGKC	3.15	Anti-rabies virus immunoglobulin rearranged kappa chain V-region
	LIN7C	3.51	lin-7 homolog C (*C. elegans*)
	LOC54499	2.31	Putative membrane protein
	M6PR	3.59	Mannose-6-phosphate receptor
	MGC8902	2.27	Hypothetical protein MGC8902/
	MOBK1B	2.67	MOB1, Mps one binder kinase activator-like 1B (yeast)
	NS	2.15	Nucleostemin
	NUSAP1	3.25	Nucleolar and spindle associated protein 1
	OK/SW-cl.56	1.85	Beta 5-tubulin
	OPRS1	2.76	Opioid receptor, sigma 1
	PEG 10	2.50	Paternally expressed 10
	PEX19	2.34	Peroxisomal biogenesis factor 19
	PGK1	2.11	Phosphoglycerate kinase 1
	RPE	2.35	Ribulose-5-phosphate-3-epimerase
	SDBCAG84	3.16	Serologically defined breast cancer antigen 84
	SMU1	2.70	smu-1 suppressor of mec-8 and unc-52 homolog (*C. elegans*)
	TAGLN2	2.03	Transgelin 2
	UBC	2.65	Ubiquitin C
	XPNPEP1	2.84	X-prolyl aminopeptidase
	YWHAE	6.39	Tyrosine 3-monooxygenase/tryptophan 5-monooxygenase activation protein, epsilon polypeptide
	YWHAZ	2.50	Tyrosine 3-monooxygenase/tryptophan 5-monooxygenase activation protein, zeta polypeptide

of $KBrO_3$ predominantly causes gross structural changes rather than small genetic changes such as point mutations.

$KBrO_3$ generates high yields of 8OHdG DNA adducts, which is a marker of oxidative DNA damage widely used as a predictor of carcinogenesis [10]. 8OHdG has been reported to be highly mutagenic in some experiments. In cell-free system, 8OHdG induced mutation by misincorporating adenine instead of cytosine [12]. Artificially incorporated 8OHdG at specific codons in a shuttle vector system efficiently induced GC > TA transversions in mammalian cells and *E. coli* [8,32,33]. In mammalian gene mutation assays in vitro and in vivo, however, the relationship between the accumulation of 8OHdG and the induction of GC > TA transversion has not been clear. Takeuchi et al.

Table 3
Genes whose expression was down-regulated by $KBrO_3$ (2.5 mM, 4 h)

	Gene symbol	Ratio	Gene title
Cell cycle, cell growth	FH	0.51	Fumarate hydratase
	MYC	0.55	v-myc myelocytomatosis viral oncogene homolog
Signal transduction	DUSP2	0.37	Dual specificityphosphatase 2
	RRBP1	0.39	Ribosome binding protein 1 homolog 180 kDa
	TBL3	0 43	Transducin (beta)-like3
Transcription regulation	CITED2	0.45	Cbp/p300-interacting transactivator, with Glu/Asp-rich carboxy-terminal domain, 2
	KIAA1196	0.43	KIAA1196 protein
	TZFP	0 39	Testis zinc finger protein
Chromosome organization	H1FX	0.14	H1 histone family member X
Protein modification	CLTB	0.43	Clathrin, light polypeptide (Lcb)
Energy pathway	FDX1	0.45	Ferredoxin 1
	QPRT	0.41	Quinolinate phosphoribosyltransferase
	SLC39A4	0.43	Solute carrier family 39 (zinc transporter), member 4
Unclassified	BTBD2	0.35	BTB (POZ) domain containing 2
	LOC339229	0.44	Hypothetical protein LOC339229
	MGRN1	0.44	Mahogunin, ring finger 1
	MRP63	0.41	Mitochondrial ribosomal protein 63
	PHLDA1	0.43	Pleckstrin homology-like domain, family A, member 1
	PTPLA	0.37	Protein tyrosine phosphatase-like (proline instead of catalytic arginine), member a
	SPATA2	0.45	Spermatogenesis associated 2

examined the mutagenicity of a hydroxyl radical generator, *N,N'*-bis (2-hydroxyperoxy-2-methoxyethyl)-1,4,5,8-naphthalene-tetra-carboxylic diimide (NP-III). Although NP-III highly produced 8OHdG upon irradiation with UV in V79 cells, the frequency of *Hprt* gene mutation was not significantly induced [34]. Molecular analysis demonstrated the no association of induction of 8OHdG with GC > TA transversion in the *Hprt* mutants [35]. 8OHdG is mainly removed by Ogg1 protein in a manor of the base excision repair (BER) pathway. Arai et al. investigated the relationship between the accumulation of oxidative DNA damage and the induction of gene mutation using *Ogg*1 deficient transgenic mice [36]. Although the 8OHdG level in kidneys of the *Ogg*1 deficient mice increase 200 times of the control level after 4 weeks' $KBrO_3$ treatment, the mutation frequency in the transgenic *gpt* gene was induced by less than 10 times of the control level. The molecular analysis revealed that the fraction of GC > TA transversions did not specifically increased. These results suggest that 8OHdG-mediated base substitutions do not mainly contribute to the mutagenic process involved in $KBrO_3$-induced carcinogenesis. Other genotoxic events must be involved in the carcinogenic process.

Our present studies strongly support this hypothesis. We demonstrated that $KBrO_3$ treatment clearly induced DNA damage in both the alkaline and neutral COM assay (Fig. 1). The alkaline COM assay is capable of detecting any DNA damages including DSB, single strand breaks (SSB), alkali-labile sites, DNA–DNA/DNA–protein cross-linking, and SSB associated with incomplete excision repair sites, while the neutral COM assay allows the detection of DSB, considered to be "biologically relevant" lesion of radiation damage [24]. $KBrO_3$ may have radio-mimic genotoxicity that yields oxidative DNA damage as well as DSB. $KBrO_3$ also induced MN formation and *TK* gene mutation significantly in TK6 cells. In the *TK* gene mutation assay, $KBrO_3$ predominantly produced SG mutants, but not NG mutants (Fig. 1c), implying that gross structural changes such as deletion and recombination are associated with the mutations. Molecular analysis of the *TK* mutants confirmed the assumption. Most of *TK* mutants showed LOH mutations, not non-LOH mutations, which are mainly point mutations. Harrington-Brock et al. also demonstrated that bromate compounds significantly induced *Tk* mutations in mouse lymphoma L5178Y cells, and almost all were LOH mutations [5]. LOH can be caused by deletions,

mitotic recombination between homologous alleles, or whole chromosome loss [20]. Molecular analysis can distinguish between them and reveal the mechanism and the characteristics of the mutants. In this study, $KBrO_3$ predominantly induced large deletions that resulted in hemizygous LOH (Table 1). The large deletions were mainly terminal deletions in the proximal region of chromosome 17q, which were rarely observed in spontaneously arising *TK* mutants (Fig. 3). The mutational spectrum and LOH pattern induced by $KBrO_3$ were similar to those induced by X-irradiation (Figs. 2 and 3) [20,21]. DSBs induced X-rays cause large deletions [19,20]. When the DSBs are repaired by the non-homologous end-joining pathway, interstitial deletions result. The broken chromosome ends can be also stabilized by the addition of new telomere sequences. Because TK6 cells have high telomerase activity [20], the result is terminal deletions. Thus, the major genotoxicity of $KBrO_3$ may be due to DSBs, but not to 8OHdG converting GC > TA transversion.

Some 8OHdG lesions can convert DSBs through the BER pathway [37]. In the initial step of BER, Ogg1 removes 8OHdG by DNA glycosylase activity and nicks the DNA backbone because of its associated lyase activity. The resulting SSB is processed by an apurinic endonuclease, which generates a single nucleotide gap. The gap is filled in by a DNA polymerase and sealed by a DNA ligase [38]. Clustered 8OHdG lesions induced by $KBrO_3$ may not be appropriately repaired by BER and cause DSB, however, because it is possible that two closely opposed 8OHdGs convert two closely opposed SSBs by BER resulting DSB [39,40]. Yang et al. developed Ogg1 over-expressing TK6 cell (TK6-hOGG1) and examined cytotoxic and mutagenic responses to gamma-irradiation [41]. They demonstrated that TK6-hOGG1 cells are more sensitive than the parental TK6 cells to cytotoxicity and mutagenicity by gamma-irradiation, and most of the induced *TK* mutants in TK6-OGG1 exhibited SG phenotype, which were probably large deletion mutants resulted by DSBs. This result clearly indicates that BER pathway contributes to convert oxidative damages to DSBs. Some clustered 8OHdG induced by $KBrO_3$ may covert to DSBs in TK6 cells, because TK6 is Ogg1 proficient cells [37].

To clarify the genotoxic characteristics of $KBrO_3$, we investigated the gene expression profile using Affymetrix GeneChip® Expression analysis. Many genes were up- or down-regulated by exposure to 2.5 mM $KBrO_3$ (Tables 2 and 3). Akerman et al. investigated the alterations of gene expression profiles in ionizing radiation-exposed TK6 cells [42]. They reported a >50% increase in expression of ATF-3 (stress response), Cyclin G (cell cycle), FAS antigen (apoptosis), GADD45 (repair and apoptosis), PCNA (repair), Rad51 (repair), and p21 (cell cycle) and a 40% decrease in expression of c-Myc (transcription factor), interferon stimulatory gene factor-3 (cell signaling), and p55CDC (cell cycle). We also observed up-regulation of p21 and down-regulation of c-Myc. Up-regulation of p21, however, is observed in TK6 cells exposed to any DNA-damaging chemical [43]. Islaih et al. also demonstrated the relationship between the gene expression profiles and the DNA damaging agents using TK6 cells [43]. They examined six chemicals including H_2O_2 and bleomycin which induce oxidative DNA damage. Although 10 genes were commonly up-regulated between H_2O_2 and bleomycin treatments, these genes except for p21 were not observed in our experiment. Thus, we could not find the similarity of gene expression profile by the treatment with $KBrO_3$ to by the treatment with ionizing radiation as well as oxidative damage inducers. Comparing gene expression profiles across platforms, laboratories, and experiments must be difficult [44]. Although it is difficult to judge from the expression analysis of the single chemical, information on genes which altered their expression gives a clue to understand the mechanism of action. Firstly, predominance of DNA repair and cell cycle related genes in up-regulated genes supports the genotoxic action of $KBrO_3$. Up-regulation of stress genes and apoptosis related genes suggests an involvement of oxidative stress. Up-regulation of catalase may be responsible for the oxidative damage by $KBrO_3$ (Table 2). Unclassified genes for alteration may have a functional relationship with genotoxic mechanism.

In conclusion, $KBrO_3$ predominantly induced large deletions at chromosomal level in human TK6 cells. The major genotoxicity leading to carcinogenesis of $KBrO_3$ may be due to DSBs rather than to 8OHdG adducts that lead to GC > TA transversions, as is commonly believed.

Acknowledgments

The TK6 cell line used in this study was a kind gift of Dr. John B. Little of the Harvard School of Public Health, Boston, MA. This study was supported by Health, Welfare, and Labor Science Research Grants (H15-chem-002, H15-food-004) in Japan.

References

[1] Y. Kurokawa, A. Maekawa, M. Takahashi, Y. Hayashi, Toxicity and carcinogenicity of potassium bromate—a new renal carcinogen, Environ. Health Perspect. 87 (1990) 309–335.

[2] Y. Kurokawa, S. Aoki, Y. Matsushima, N. Takamura, T. Imazawa, Y. Hayashi, Dose–response studies on the carcinogenicity of potassium bromate in F344 rats after long-term oral administration, J. Natl. Cancer Inst. 77 (1986) 977–982.
[3] A.B. DeAngelo, M.H. George, S.R. Kilburn, T.M. Moore, D.C. Wolf, Carcinogenicity of potassium bromate administered in the drinking water to male B6C3F1 mice and F344/N rats, Toxicol. Pathol. 26 (1998) 587–594.
[4] M. Ishidate Jr., K. Yoshikawa, Chromosome aberration tests with Chinese hamster cells in vitro with and without metabolic activation—a comparative study on mutagens and carcinogens, Arch. Toxicol. Suppl. 4 (1980) 41–44.
[5] K. Harrington-Brock, D.D. Collard, T. Chen, Bromate induces loss of heterozygosity in the thymidine kinase gene of L5178Y/Tk(±)-3.7.2C mouse lymphoma cells, Mutat. Res. 537 (2003) 21–28.
[6] M. Hayashi, T. Sofuni, M. Ishidate Jr., High-sensitivity in micronucleus induction of a mouse strain (MS), Mutat. Res. 105 (1982) 253–256.
[7] M. Hayashi, M. Kishi, T. Sofuni, M. Ishidate Jr., Micronucleus tests in mice on 39 food additives and eight miscellaneous chemicals, Food Chem. Toxicol. 26 (1988) 487–500.
[8] H. Kamiya, K. Miura, H. Ishikawa, H. Inoue, S. Nishimura, E. Ohtsuka, c-Ha-ras containing 8-hydroxyguanine at codon 12 induces point mutations at the modified and adjacent positions, Cancer Res. 52 (1992) 3483–3485.
[9] A.G. Knudson, Antioncogenes and human cancer, Proc. Natl. Acad. Sci. U.S.A. 90 (1993) 10914–10921.
[10] H. Kasai, S. Nishimura, Y. Kurokawa, Y. Hayashi, Oral administration of the renal carcinogen, potassium bromate, specifically produces 8-hydroxydeoxyguanosine in rat target organ DNA, Carcinogenesis 8 (1987) 1959–1961.
[11] K.C. Cheng, D.S. Cahill, H. Kasai, S. Nishimura, L.A. Loeb, 8-Hydroxyguanine, an abundant form of oxidative DNA damage, causes G–T and A–C substitutions, J. Biol. Chem. 267 (1992) 166–172.
[12] S. Shibutani, M. Takeshita, A.P. Grollman, Insertion of specific bases during DNA synthesis past the oxidation-damaged base 8-oxodG, Nature 349 (1991) 431–434.
[13] K. Sai, C.A. Tyson, D.W. Thomas, J.E. Dabbs, R. Hasegawa, Y. Kurokawa, Oxidative DNA damage induced by potassium bromate in isolated rat renal proximal tubules and renal nuclei, Cancer Lett. 87 (1994) 1–7.
[14] G. Speit, S. Haupter, P. Schutz, P. Kreis, Comparative evaluation of the genotoxic properties of potassium bromate and potassium superoxide in V79 Chinese hamster cells, Mutat. Res. 439 (1999) 213–221.
[15] T. Umemura, K. Sai, A. Takagi, R. Hasegawa, Y. Kurokawa, A possible role for oxidative stress in potassium bromate (KBrO3) carcinogenesis, Carcinogenesis 16 (1995) 593–597.
[16] K. Fujie, H. Shimazu, M. Matsuda, T. Sugiyama, Acute cytogenetic effects of potassium bromate on rat bone marrow cells in vivo, Mutat. Res. 206 (1988) 455–458.
[17] M. Ishidate Jr., T. Sofuni, K. Yoshikawa, M. Hayashi, T. Nohmi, M. Sawada, A. Matsuoka, Primary mutagenicity screening of food additives currently used in Japan, Food Chem. Toxicol. 22 (1984) 623–636.
[18] H.L. Liber, W.G. Thilly, Mutation assay at the thymidine kinase locus in diploid human lymphoblasts, Mutat. Res. 94 (1982) 467–485.
[19] H.L. Liber, D.W. Yandell, J.B. Little, A comparison of mutation induction at the tk and hprt loci in human lymphoblastoid cells: quantitative differences are due to an additional class of mutations at the autosomal tk locus, Mutat. Res. 216 (1989) 9–17.
[20] M. Honma, Generation of loss of heterozygosity and its dependency on p53 status in human lymphoblastoid cells, Environ. Mol. Mutagen. 45 (2005) 162–176.
[21] M. Honma, M. Hayashi, T. Sofuni, Cytotoxic and mutagenic responses to X-rays and chemical mutagens in normal and p53-mutated human lymphoblastoid cells, Mutat. Res. 374 (1997) 89–98.
[22] L. Zhan, H. Sakamoto, M. Sakuraba, D.S. Wu, L.S. Zhang, T. Suzuki, M. Hayashi, M. Honma, Genotoxicity of microcystin-LR in human lymphoblastoid TK6 cells, Mutat. Res. 557 (2004) 1–6.
[23] N. Koyama, H. Sakamoto, M. Sakuraba, T. Koizumi, Y. Takashima, M. Hayashi, H. Matsufuji, K. Yamagata, S. Masuda, N. Kinae, M. Honma, Genotoxicity of acrylamide and glycidamide in human lymphoblastoid TK6 cells, Mutat. Res. 603 (2006) 151–158.
[24] S. Wada, H. Kurahayashi, Y. Kobayashi, T. Funayama, K. Yamamoto, M. Natsuhori, N. Ito, The relationship between cellular radiosensitivity and radiation-induced DNA damage measured by the comet assay, J. Vet. Med. Sci. 65 (2003) 471–477.
[25] M. Watanabe-Akanuma, T. Ohta, Y.F. Sasaki, A novel aspect of thiabendasole as a photomutagen in bacteria and cultured human cells, Mutat. Res. 158 (2005) 213–219.
[26] T. Matsushima, M. Hayashi, A. Matsuoka, M. Ishidate Jr., K.F. Miura, H. Shimizu, Y. Suzuki, K. Morimoto, H. Ogura, K. Mure, K. Koshi, T. Sofuni, Validation study of the in vitro micronuclei test in a Chinese hamster lung cell line (CHL/IU), Mutagenesis 14 (1999) 569–580.
[27] T. Omori, M. Honma, M. Hayashi, Y. Honda, I. Yoshimura, A new statistical method for evaluating of L5178Ytk± mammalian cell data using microwell method 517 (2002) 199–208.
[28] M. Honma, M. Momose, H. Tanabe, H. Sakamoto, Y. Yu, J.B. Little, T. Sofuni, M. Hayashi, Requirement of wild-type p53 protein for maintenance of chromosomal integrity, Mol. Carcinog. 28 (2000) 203–214.
[29] P.L. Olive, DNA damage and repair in individual cells: applications of the comet assay in radiobiology, Int. J. Radiat. Biol. 75 (1999) 395–405.
[30] D.E. Levin, M. Hollstein, M.F. Christman, E.A. Schwiers, B.N. Ames, A new Salmonella tester strain (TA102) with A X T base pairs at the site of mutation detects oxidative mutagens, Proc. Natl. Acad. Sci. U.S.A. 79 (1982) 7445–7449.
[31] T. Arai, V.P. Kelly, O. Minowa, T. Noda, S. Nishimura, High accumulation of oxidative DNA damage, 8-hydroxyguanine, in Mmh/Ogg1 deficient mice by chronic oxidative stress, Carcinogenesis 23 (2002) 2005–2010.
[32] F. Le Page, A. Margot, A.P. Grollman, A. Sarasin, A. Gentil, Mutagenicity of a unique 8-oxoguanine in a human Ha-ras sequence in mammalian cells, Carcinogenesis 16 (1995) 2779–2784.
[33] M.L. Wood, M. Dizdaroglu, E. Gajewski, J.M. Essigmann, Mechanistic studies of ionizing radiation and oxidative mutagenesis: genetic effects of a single 8-hydroxyguanine (7-hydro-8-oxoguanine) residue inserted at a unique site in a viral genome, Biochemistry 29 (1990) 7024–7032.
[34] T. Takeuchi, S. Matsugo, K. Morimoto, Mutagenicity of oxidative DNA damage in Chinese hamster V79 cells, Carcinogenesis 18 (1997) 2051–2055.
[35] M. Nakajima, T. Takeuchi, K. Ogino, K. Morimoto, Lack of direct involvement of 8-hydroxy-2′-deoxyguanosine in

hypoxanthine-guanine phosphoribosyltransferase mutagenesis in V79 cells treated with *N,N'*-bis(2-hydroxyperoxy-2-methoxy-ethyl)-1,4,5,8-naphthalenetetracarboxyli c-diimide (NP-III) or riboflavin, Jpn. J. Cancer Res. 93 (2002) 247–252.

[36] T. Arai, V.P. Kelly, K. Komoro, O. Minowa, T. Noda, S. Nishimura, Cell proliferation in liver of Mmh/Ogg1-deficient mice enhances mutation frequency because of the presence of 8-hydroxyguanine in DNA, Cancer Res. 63 (2003) 4287–4292.

[37] N. Yang, M.A. Chaudhry, S.S. Wallace, Base excision repair by hNTH1 and hOGG1: a two edged sword in the processing of DNA damage in gamma-irradiated human cells, DNA Repair (Amst.) 5 (2006) 43–51.

[38] G. Slupphaug, B. Kavli, H.E. Krokan, The interacting pathways for prevention and repair of oxidative DNA damage, Mutat. Res. 531 (2003) 231–251.

[39] K. Tian, M. McTigue, S.C. de los, Sorting the consequences of ionizing radiation: processing of 8-oxoguanine/abasic site lesions, DNA Repair (Amst.) 1 (2002) 1039–1049.

[40] M.E. Lomax, S. Cunniffe, P. O'Neill, Efficiency of repair of an abasic site within DNA clustered damage sites by mammalian cell nuclear extracts, Biochemistry 43 (2004) 11017–11026.

[41] N. Yang, H. Galick, S.S. Wallace, Attempted base excision repair of ionizing radiation damage in human lymphoblastoid cells produces lethal and mutagenic double strand breaks, DNA Repair (Amst.) 3 (2004) 1323–1334.

[42] G.S. Akerman, B.A. Rosenzweig, O.E. Domon, C.A. Tsai, M.E. Bishop, L.J. McGarrity, J.T. Macgregor, F.D. Sistare, J.J. Chen, S.M. Morris, Alterations in gene expression profiles and the DNA-damage response in ionizing radiation-exposed TK6 cells, Environ. Mol. Mutagen. 45 (2005) 188–205.

[43] M. Islaih, B.W. Halstead, I.A. Kadura, B. Li, J.L. Reid-Hubbard, L. Flick, J.L. Altizer, D.J. Thom, D.K. Monteith, R.K. Newton, D.E. Watson, Relationships between genomic, cell cycle, and mutagenic responses of TK6 cells exposed to DNA damaging chemicals, Mutat. Res. 578 (2005) 100–116.

[44] C.L. Yauk, M.L. Berndt, A. Williams, G.R. Douglas, Comprehensive comparison of six microarray technologies, Nucleic Acids Res. 32 (2004) e124.

MOLECULAR AND CELLULAR BIOLOGY, Aug. 2007, p. 5261–5274 Vol. 27, No. 15
0270-7306/07/$08.00+0 doi:10.1128/MCB.01852-06

Interchromosomal Crossover in Human Cells Is Associated with Long Gene Conversion Tracts▽

Efrem A. H. Neuwirth,[1] Masamitsu Honma,[2] and Andrew J. Grosovsky[1]*

Department of Cell Biology and Neuroscience and Environmental Toxicology Graduate Program, University of California, Riverside, California 92521,[1] and Division of Genetics and Mutagenesis, National Institute of Health Sciences, Setagaya, Tokyo, Japan[2]

Received 30 September 2006/Returned for modification 2 November 2006/Accepted 23 April 2007

Crossovers have rarely been observed in specific association with interchromosomal gene conversion in mammalian cells. In this investigation two isogenic human B-lymphoblastoid cell lines, TI-112 and TSCER2, were used to select for I-SceI-induced gene conversions that restored function at the selectable thymidine kinase locus. Additionally, a haplotype linkage analysis methodology enabled the rigorous detection of all crossover-associated convertants, whether or not they exhibited loss of heterozygosity. This methodology also permitted characterization of conversion tract length and structure. In TI-112, gene conversion tracts were required to be complex in tract structure and at least 7.0 kb in order to be selectable. The results demonstrated that 85% (39/46) of TI-112 convertants extended more than 11.2 kb and 48% also exhibited a crossover, suggesting a mechanistic link between long tracts and crossover. In contrast, continuous tracts as short as 98 bp are selectable in TSCER2, although selectable gene conversion tracts could include a wide range of lengths. Indeed, only 16% (14/95) of TSCER2 convertants were crossover associated, further suggesting a link between long tracts and crossover. Overall, these results demonstrate that gene conversion tracts can be long in human cells and that crossovers are observable when long tracts are recoverable.

In mammalian cells, gene conversion without associated crossover has been widely reported for both intrachromosomal and interchromosomal recombining substrates (13, 51, 62, 80, 87). However, most studies to date have not succeeded in associating interchromosomal crossovers with specific conversion tracts (37, 67, 71, 80, 83); reports of crossovers are rare (7, 72). Nevertheless, presumptive interchromosomal crossovers, in the form of chromosome-scale loss of heterozygosity (LOH), are commonly observed in mammalian cells. LOH is the major contributor to the mutational spectrum in mice and humans (31, 33, 47, 49, 78), notably at tumor suppressor loci (3, 11, 15, 25, 34, 35, 40, 68, 88, 89). Crossover products have also been associated with intrachromosomal recombination between repeat sequences in mammalian cells (12, 30, 52, 75), and similar outcomes are observed during the integration of plasmids into host cell chromosomes (9, 48, 90). Additional evidence for crossovers in mammalian cells is provided by the relatively frequent occurrence of sister chromatid exchange (94), although these products may also result from other mechanisms (56). Since the occurrence of crossovers in mammalian cells has been clearly demonstrated, the absence of crossovers associated with specific interchromosomal gene conversion tracts requires further explanation.

Several mechanisms have been proposed to explain the preference for gene conversion without associated crossover in eukaryotic organisms. Crossover is believed to require the formation of Holliday intermediates (17, 36, 44, 76, 77) and their resolution through structure-specific endonuclease scissions (79). Theoretically, half of Holliday junctions that are resolved through scissions would be cut in a configuration that results in crossover (36). However, crossovers can be precluded by well-described recombinational pathways that do not meet these requirements. For example, recombinational exchanges may occur through synthesis-dependent strand annealing (24, 63, 65), in which strand invasion intermediates are removed following repair synthesis but before Holliday junctions can form, thus partially accounting for the absence of associated crossovers. Once formed, Holiday junctions can be resolved without endonuclease scissions, through the unwinding action of a complex involving topoisomerase III and a RecQ family helicase such as BLM (95). A third possibility is that endonuclease resolution inherently favors scissions in a configuration leading to noncrossovers (18). Furthermore, crossovers may require steps that can be suppressed, such as structural isomerization (80). Branch migration, which may facilitate isomerization, also presents a target for regulation (58, 81).

In yeast, the paucity of mitotic interchromosomal crossovers is correlated with the prevalent occurrence of short conversion tracts, suggesting a mechanistic link. One early study reported that specific selection for long, complex conversion tracts resulted in a very high crossover association (73). Furthermore, crossovers are disproportionately associated with relatively rare long tracts in intrachromosomal or plasmid-based systems (1, 2), and a reduction in the overall length of available homology has been found to reduce interchromosomal crossovers to a much greater extent than gene conversion (39, 41). Enzymatic functions which have differential effects on gene conversion and crossover have also been shown to influence conversion tract length (1, 10, 53, 55, 85), thus supporting the hypothesis that the occurrence of crossover is linked to tract length.

In this investigation we evaluated the hypothesis that tract length will also be one of the primary determinants of cross-

* Corresponding author. Mailing address: University of California, Department of Cell Biology and Neuroscience, 2211 Biological Sciences Building, Riverside, CA 92521. Phone: (951) 827-3193. Fax: (951) 827-3087. E-mail: grosovsky@ucr.edu.

▽ Published ahead of print on 21 May 2007.

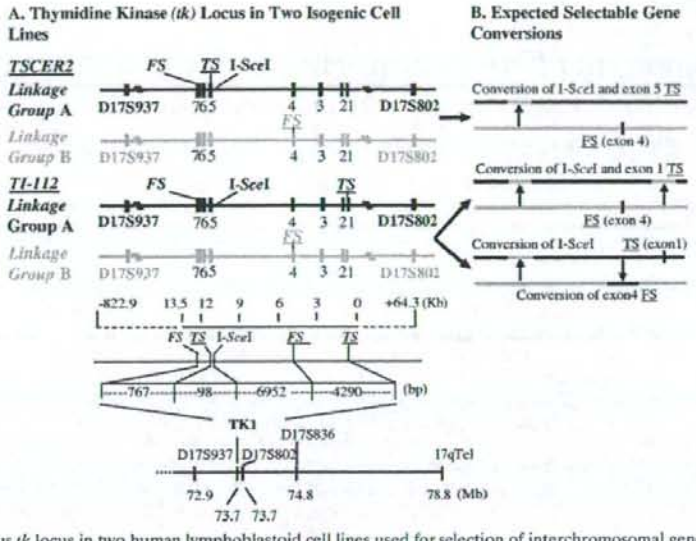

FIG. 1. The endogenous *tk* locus in two human lymphoblastoid cell lines used for selection of interchromosomal gene conversion and expected conversion patterns. (A) Maps of the *tk* gene in cell lines TSCER2 and TI-112. Exons are shown as vertical bars, and the relative positions of the *tk* gene and flanking microsatellite loci are shown according to scale. Intragenic polymorphic markers are shown in bold, and the *tk*-inactivating mutations are underlined. Three polymorphisms in the coding portion of the gene used for analysis are common to both cell lines: an inactivating FS insertion at exon 4 on allele B, a silent FS insertion in exon 7 on allele A, and a 31-bp insertion containing the I-SceI recognition sequence in intron 4. The two cell lines differ for the *tk*-inactivating mutation on allele A. TSCER2 has a TS mutation in exon 5. TI-112 has a TS mutation in exon 1. The parental linkage groups are defined as A or B and are shown in black or gray, respectively. Polymorphisms at the flanking polymorphic microsatellites D17S937, D17S802, and D17836 depicted here were also analyzed to determine the extent of LOH and establish linkage relationships. Physical distances between each marker are presented, as are the positions of the TK1 locus and flanking markers on chromosome 17q. (B) The expected gene conversion patterns from the two cell lines are depicted. Both cell lines could also be restored by a switch in linkage between the two inactivating mutations (not shown).

over association in mammalian cells. This issue has been addressed in an intrachromosomal recombination study (30), but no systematic analysis for interchromosomal recombination has been previously reported. In order to study the crossover association of interchromosomal gene conversion in human cells, we employed a haplotype linkage analysis (HLA) methodology (67). The HLA approach enabled linkage determinations within the selectable locus, as well as for flanking heterozygous loci within a study region of 1.9 megabases. For this investigation we developed a pair of isogenic cells lines, each of which contains an I-SceI endonuclease recognition sequence within the endogenous thymidine kinase (*tk*) locus. In cell line TI-112, where selectable conversion tracts must be a minimum of 7.0 kb in length and complex in tract structure, the crossover association was 48%. In contrast, cell line TSCER2 (37) permits a wider range of selectable conversion tract lengths, including continuous tracts as short as 98 bp; the crossover association in this system was 16%. In some cases, the HLA system also permitted the identification of unselected conversion tracts that were cosegregated into convertant clones with selected conversion tracts. These unselected conversion tracts were often long, even though length was not a prerequisite for their recovery, thus suggesting that tracts of 7 kb and longer can frequently occur in interchromosomal recombination. These results demonstrate that even in the absence of selection, crossovers are particularly associated with long conversion tracts in human cells. The observation of crossovers in the present investigation, which is in contrast to a previous study of this issue (83), is due to the robust ability of the experimental system to recover and fully analyze long and complex conversion tracts.

MATERIALS AND METHODS

Cell lines used and locations of polymorphic markers. The TK6 cell line (50) is a well-characterized human B-lymphoblastoid cell line that is functionally heterozygous at the *tk* locus. The human *tk* locus is located on chromosome 17q, 73.7 Mb from 17pTel and 5.1 Mb from 17qTel (46). The gene is 12.9 kb long with 702 bp of coding region (14, 26) and codes for a protein involved in a salvage pathway for dTTP biosynthesis. Forward selection to TK^- can be accomplished using trifluorothymidine (TfT) (82), and reversion to TK^+ can be obtained using cytidine, hypoxanthine, aminopterin, and thymidine (CHAT) (16, 50).

Cell lines TSCER2 and TI-112 are isogenic $tk^{-/-}$ derivatives of TK6. The structures of the *tk* locus in the two cell lines are shown in Fig. 1, with the transcriptional direction towards the centromere as shown by human genome sequencing (46). TK6 is mutated in exon 4 of allele B of the *tk* gene, with a single-base C frameshift (FS) insertion in a run of three Cs at position 4864 of the genomic DNA sequence. There is a phenotypically silent FS insertion on allele A in a run of four Gs at position 12690 in exon 7 (32). TSCER2 was generated as described previously (37). In brief, a two-step gene targeting was performed to introduce an I-SceI site into intron 4 of TK6 to create cell line TSCE5. The 31-bp I-SceI recognition sequence and linker DNA are located in a BglII site at positions 11815 to 11820. Cell lines TSCER2 and TI-112 are TfT-resistant spontaneous $tk^{-/-}$ mutants of TSCE5. TSCER2 is mutated in position 11923, with a G-to-A transition (TS) resulting in a change of codon from a TGC (cysteine) to TAC (tyrosine). TI-112, newly collected for this study, has a G-to-A TS at

position 574 resulting in a codon change of GGG (glycine) to AGG (arginine). Cell lines were maintained in RPMI 1640 with 10% iron-supplemented calf serum, 1% L-glutamine, and 1% penicillin-streptomycin mix and cultured at 37°C with 5% CO_2 with the cell density kept between 2×10^5 and 10×10^5 cells/ml.

Frequency determinations and collection of independent revertants. TI-112 and TSCER2 cells were pretreated with 2 μg/ml TfT for 2 days to remove preexisting revertants and expanded to a minimum of 1×10^7 cells/flask. Cells were electroporated using the AMAXA Biosystems electroporator, program A30, in company-provided solution V using recommended cell preparation and conditions. For both frequency determinations and independent revertant collections, 1×10^7 cells were electroporated with 20 μg I-SceI expression vector pCBASce (71). Immediately following electroporation, the cells were separated into 10 to 20 flasks for collecting independent revertants. Following a phenotypic expression and cell recovery period of 4 to 5 days cells, were plated in CHAT medium to select for TK^+ revertants. Control cells were untreated and maintained alongside the treated cells. TSCER2 cells were plated at a concentration of 1×10^4 cells/well, and TI-112 cells at 4×10^4 cells/well, in 96-well plates. Plates were scored on days 12 to 14 for normal-growth revertants and also on days 21 and 28 for slow-growth revertants. This slow-growth phenotype is presumed to be due to a *tk*-linked gene near the telomere on 17q, which specifically shows a slow-growth phenotype when this gene becomes coordinately homozygous with *tk* allele B (4, 5). TSCER2 colonies were subcloned to ensure that colonies derived from single TK convertants. TI-112 convertants occurred at lower frequencies and so did not require subcloning to ensure independence.

Collection of HLA clones. The collection of clones for HLA was performed as previously described (67). In brief, for each convertant clone, a small set of spontaneous TfT-resistant mutants was collected and analyzed for LOH at the flanking microsatellite loci in order to identify at least one clone that was coordinately LOH at *tk*-flanking microsatellite markers D17S937, D17S802, and D17S836. This convertant was used for all subsequent haplotype analyses.

Genomic analysis of TK convertant and derivative haplotype clones. DNA purification and PCR of *tk* intragenic and flanking microsatellite markers was performed as previously described (28, 32, 67). The PCR products containing the intragenic *tk* markers were sequenced by capillary electrophoresis (ABI) and visualized using standard software (Chromas). Primers were obtained from Invitrogen Inc.

RESULTS

Overview of experimental system. This study was designed to define the spectrum of gene conversion events in an isogenic pair of human lymphoblastoid cell lines, including the fraction of conversions that are associated with crossover, as well as the lengths and internal structures of conversion tracts. The cell lines used for this analysis differ only in the placement of inactivating mutations in the *tk* locus (Fig. 1A). In cell line TI-112, there are no continuous tracts that are selectable. Only very long (7 or 11.2 kb) and complex conversion tracts can be selected (Fig. 1B). Recoverable complex conversion tracts include conversion of the I-SceI site together with conversion of the exon 4 FS on the donor allele, discontinuous conversion of the more distal exon 1 TS, or a switch in linkage between these two inactivating mutations without conversion of either marker. Continuous conversion tracts extending through the exon-inactivating FS mutation (Fig. 1A) would result in a homozygous mutant, which would not be a selectable outcome. With the TSCER2 cell line, there are five possible continuous tracts involving the four intragenic markers, but only two are TK^+ and selectable (Fig. 1B): tracts from I-SceI to exon 5 (98 bp) and from I-SceI to exon 7 (865 bp). These tract lengths are minimal. Longer tracts that extend beyond the intragenic markers could also be recoverable, except those that involve coconversion of the exon 4 FS. The overlapping capabilities of these two cell lines provide a broad window for construction of a comprehensive spectrum of gene conversion tracts.

Using these cell lines and HLA (see below), convertants

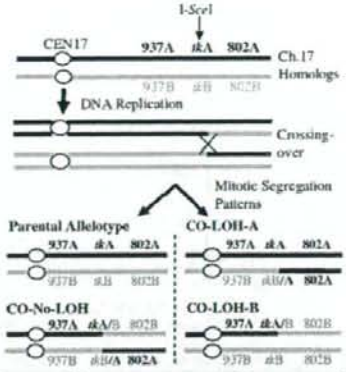

FIG. 2. Recoverable crossover patterns. Crossover and subsequent mitotic segregation can produce three detectable allelotype patterns (conversion without accompanying crossover [No-CO] is not shown here). Crossover without flanking marker LOH (CO-No-LOH) occurs when the crossed-over chromosomes cosegregate into the same cell. Crossover with LOH (CO-LOH) occurs when a recombinant chromosome and a nonrecombinant chromosome cosegregate into a cell to create homozygosity from the crossover point to the telomere. Two different CO-LOH patterns are recoverable, CO-LOH-A and CO-LOH-B, in which there is homozygosity of either A chromosome or B chromosome markers. The position of the I-SceI site within the *tk* allele on the A chromosome is indicated.

could be categorized as no crossover (No-CO) if LOH or linkage switches were localized to intragenic markers. A linkage switch that occurs in the absence of a crossover of flanking markers is evidence of either double-crossover resolution of flanking Holliday junctions or independent resolution of mismatches within symmetric heteroduplex DNA. In addition, all three possible single-crossover products could be unambiguously distinguished through flanking marker analysis (Fig. 2): crossover with no flanking marker LOH (CO-No-LOH) or crossover with homozygosity for telomeric microsatellite polymorphisms linked to the "A chromosome" (CO-LOH-A) or the "B chromosome" (CO-LOH-B). The A chromosome contains the I-SceI cut site and is therefore the cut chromosome, while the B chromosome is the donor chromosome. Crossovers that lead to flanking marker LOH are expected to represent half of such events, whereas the remaining half of crossovers do not produce LOH (Fig. 2). Typically, this can lead to underrepresentation of crossover estimates, although the HLA system minimizes the likelihood of a significant underestimate. Still, due to the requirements of producing a selectable outcome, some products may be underrepresented, so the crossover measurements reported here should be regarded as minimal.

HLA of conversion and crossover in human cells. The characterization of intragenic conversion tracts and the rigorous identification of crossovers were performed through HLA (Fig. 3). HLA is a stepwise process based on the ability to alternately select TK^+ and TK^- phenotypes and the frequent occurrence of multilocus LOH as a mechanism for generation of $tk^{-/-}$ mutants. Since LOH results in homozygosity for one of the parental haplotypes, the linkage relationship of every marker in that haplotype can be unambiguously established, and the

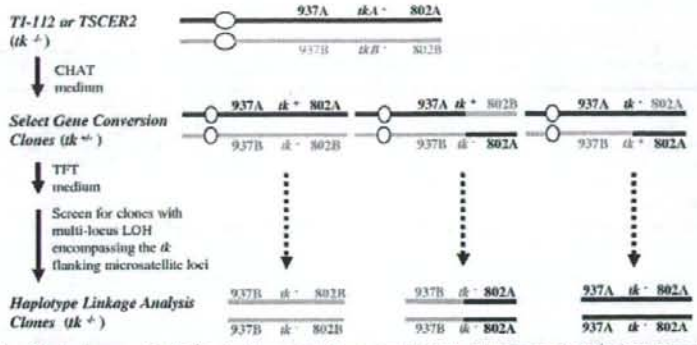

FIG. 3. Methodology for HLA. A parental $tk^{-/-}$ allelotype and three anticipated allelotypes of $tk^{+/-}$ CHAT-resistant convertants with or without crossover are depicted. A set of $tk^{-/-}$ TFT-resistant derivative clones are isolated from each convertant for the purposes of analysis only and screened for LOH encompassing flanking microsatellite markers. tk^{-} mutants are depicted as homozygous, since this is the dominant spontaneous LOH product. In several cases multiple derivative clones were analyzed, and in each case the marker patterns were the same (data not shown). The linkage relationship in the parental convertant can be established by identification of which alleles become coordinately homozygous at the flanking microsatellite loci among $tk^{-/-}$ mutants. Conservation of the parental linkage confirms the absence of crossover associated with the localized gene conversion within the *tk* locus. An altered linkage of flanking microsatellites indicates crossover.

linkage relationship for the second haplotype can be subsequently deduced. HLA begins with the selection of a small set of derivative $tk^{-/-}$ clones from each independent $tk^{+/-}$ convertant by using growth in TFT (Fig. 3). These derivative clones are then screened for LOH at flanking microsatellite markers, since a linkage switch for these distant markers can be used to establish the occurrence of crossover. Since D17S802 is relatively close to the locus (64 kb) and conceivably may be included in a conversion tract, an additional telomeric marker, D17S836, 1.1 Mb from *tk* was also examined in each clone to firmly establish crossovers. HLA analysis was routinely performed for the intragenic markers and three flanking microsatellite markers, enabling linkage relationships to be determined for a 1.9-Mb region encompassing the TK gene (Fig. 1A).

HLA was also able to demonstrate the length and complexity of intragenic conversion tracts (Fig. 4 to 6) and in some cases to discriminate cosegregating conversion tracts arising from independent I-SceI-induced breaks (Fig. 7). While this is very powerful, it also produces complex outcomes in individual clones. Still, analysis of the aggregate of convertant clones allows patterns to emerge that can be associated with specific models for recombination.

A. TI-112

	No-CO	CO-No-LOH	CO-LOH-B	CO-LOH-A	Total
Long	4	3			7
Long	9	2	3	6	20
Long	9	3	6	1	19
Total	*22*	*8*	*9*	*7*	*46*

B. TSCER2

	No-CO	CO-No-LOH	CO-LOH-B	CO-LOH-A	Total
Short				4	4
Short	37				37
Short	44	1			45
Long				4	4
Long			1	2	3
ND				2	2
Total	*81*	*1*	*1*	*12*	*95*

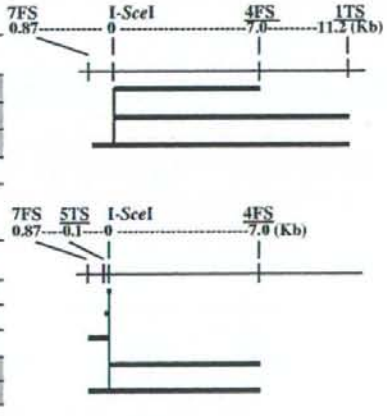

FIG. 4. Summary of conversion tract lengths from TI-112 (A) and TSCER2 (B). Conversion tract lengths represent intragenic polymorphic markers known to be included within the tract and are therefore minimal tract length estimates. These tract lengths represent both converted and unconverted markers; an intragenic marker which is unconverted is considered part of the conversion tract if it is established that the marker was between the DSB and the site of a crossover or another conversion. HLA allows the conversion tracts on both recombining alleles to be determined; for simplicity, the longer conversion tract is presented, except in the case of CO-LOH convertants, where the crossover allele is always presented. In two cases, conversion tract lengths were not determined (ND).

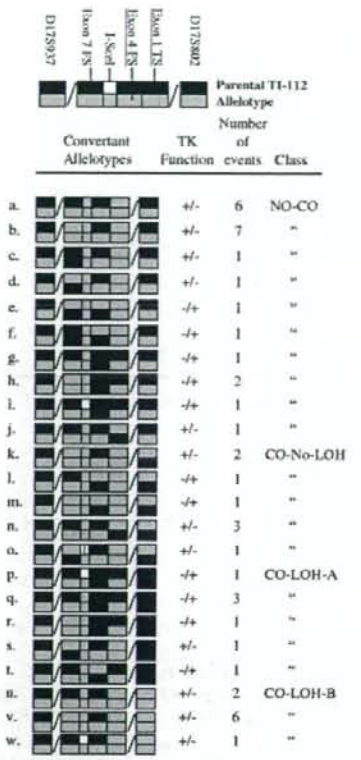

FIG. 5. TI-112 convertant allelotypes. The allelotypes for 37 normal-growth and 9 slow-growth CO-LOH-B recombinant clones are presented for two flanking and four intragenic *tk* markers. TK-inactivating mutations are underlined. Although D17S836 is not shown, it was also examined in all cases and never deviated from D17S802. Polymorphisms linked to the A chromosome are shown in black, except for the I-SceI site, which is depicted in white. Polymorphisms linked to the B chromosome are shown in gray. The single clone containing a striped I-SceI site (convertant allelotype o) represents a small deletion within the I-SceI insert. The mutant status of each *tk* allele is depicted as +/−, −/+, or +/+; these refer to the alleles on the A and B chromosome, respectively. There are multiple routes that can explain the complex patterns in any individual gene conversion tract; however, all are compatible with a model involving a double Holliday junction intermediate together with independent repair of heteroduplex positions. Changes observed on the uncut chromosome (rows c to j and l to t) offer particularly strong evidence for this hypothesis.

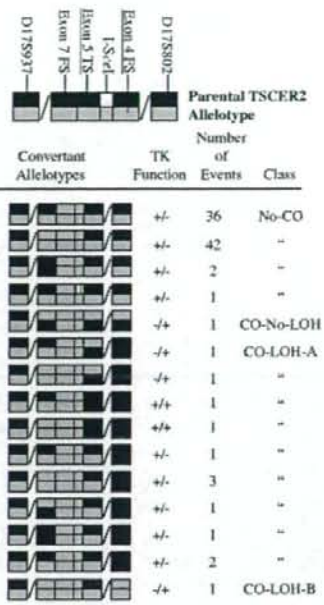

FIG. 6. TSCER2 convertant allelotypes. The allelotypes for 94 normal-growth and 1 slow-growth CO-LOH-B recombinant clones are presented for two flanking and four intragenic *tk* markers. TK-inactivating mutations are underlined. Although flanking marker D17S836 is not shown, it was also examined in all cases and never deviated from D17S802. Polymorphisms linked to the A chromosome are shown in black, except for the I-SceI insert, which is depicted in white. Polymorphisms linked to the B chromosome are shown in gray. The striped I-SceI site (convertant allelotype d) represents a small deletion/insertion event involving the I-SceI insert and several bases of flanking sequence and an insertion of two bases (GG). The mutant status of each *tk* allele is depicted as +/−, −/+, or +/+; these refer to the allele on the A and B chromosomes, respectively. The complexity seen here for CO-LOH-A convertants (rows f to n) is attributed primarily to the cosegregation of independent conversion tracts (see Fig. 7).

An estimated 48% of TI-112 convertants are associated with crossover. TI-112 convertants were recovered at a total frequency of 1.54×10^{-6} (Table 1), which represents an increase of approximately 2 orders of magnitude over the background level ($<0.06 \times 10^{-6}$). A total of 36 independent normal-growth convertants as well as 9 slow-growth convertants were collected from TI-112 for an analysis of crossover association and conversion tract spectrum. Using HLA analysis, it was determined that 48% of this set of convertants were crossovers, corresponding to a frequency of 0.74×10^{-6} (Table 1). The observed crossovers were distributed fairly evenly among each of the three crossover categories (Table 1). A summary of the conversion tract lengths by crossover classification is presented in Fig. 4A, and allelotypes for individual convertants are provided in Fig. 5.

A total of 16% of TSCER2 convertants are associated with crossover. The I-SceI-induced conversion frequency in TSCER2 was 40.7×10^{-6} (Table 1), at least 400-fold greater than background levels ($<0.1 \times 10^{-6}$) and a much greater induction than seen in TI-112. The higher induction in TSCER2 than in TI-112 may be due to the ability to produce selectable tracts in which the inactivating mutation linked to the double-strand break (DSB) can be converted in continuous tracts initiated at the DSB. In contrast, TI-112 requires a discontinuous or donor marker conversion, both of which are known to be rare (Fig. 1). A collection of 94 normal-growth convertants and one rare slow-growth convertant were obtained from TSCER2 for an analysis of crossover association and conversion tract spectrum. A total of 16% of TSCER2 convertants were associated with a crossover, which was threefold lower than the crossover fraction in TI-112 (Table 1).

A summary of the conversion tract lengths by crossover

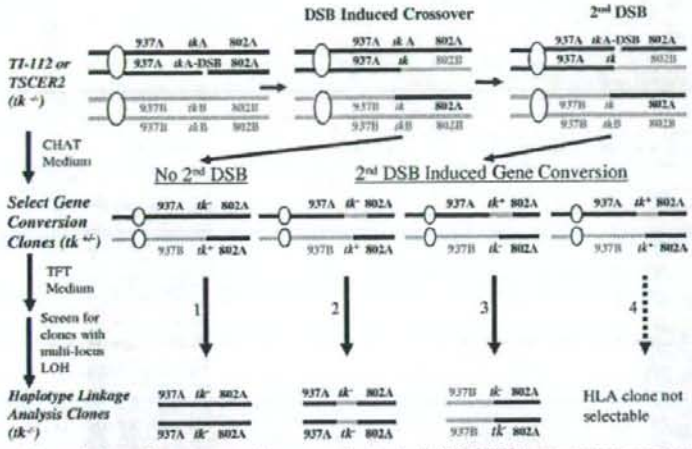

FIG. 7. HLA can distinguish two independent cosegregating conversion tracts. In CO-LOH-A convertants, a crossover *tk* allele B cosegregates with the sister chromatid *tk* allele A that was not involved in the crossover. This cosegregating allele also has an I-SceI site which may also be cut and repaired. There are four possible configurations of convertant clones, which differ depending on whether a second cut occurred and whether one or both of the cosegregating *tk* alleles were tk^+ or tk^-. Therefore, there are also four possible types of HLA clones, as shown: 1, the I-SceI site on the cosegregating noncrossover allele remains uncut; 2, the I-SceI site on the noncrossover allele is cut and repaired but the allele remains tk^-; 3, the I-SceI site on the noncrossover allele is cut and repaired, and the allele is converted to tk^+; 4, both crossover and noncrossover alleles are tk^+, precluding haplotype analysis. Only two convertants in category 4 were observed. Multiple conversion tracts can produce a tk^- or a tk^- allele.

classification is presented in Fig. 4B, and allelotypes for individual convertants are provided in Fig. 6. Most of these crossovers were determined to be associated with LOH, and in particular CO-LOH-A (Fig. 4 and Fig. 6f to n), accounting for 0.13 of all convertants (Table 1). Random mitotic segregation should lead to an equal number of crossovers without accompanying LOH (CO-No-LOH), but only 1 CO-No-LOH convertant was observed (Fig. 4 and 6e), compared to 12 CO-LOH-A convertants (Fig. 4A and 6f to n). CO-LOH-B convertants (Fig. 6o), which provide a measurement of long and discontinuous conversion tracts in TSCER2, constituted less than 0.01 of the overall spectrum (Table 1).

TABLE 1. Frequency of I-SceI-induced gene conversion and associated crossover

Event	Estimated frequency (10^{-6}) (fraction of total) in:	
	TI-112 cells	TSCER2 cells
Overall gene conversion[a]	1.54	40.72
No-CO[b]	0.80 (0.52)	34.7 (0.85)
CO-No-LOH[b]	0.29 (0.19)	0.63 (0.02)
CO-LOH-A[b]	0.26 (0.17)	5.17 (0.13)
CO-LOH-B[c]	0.19 (0.12)	0.22 (0.01)
Overall crossover[d]	0.74 (0.48)	6.03 (0.16)

[a] The overall gene conversion frequency is derived by adding the frequencies from the colony-forming assay scored on day 14 and 21 followed by verification of the drug resistance and doubling times of selected colonies. Each frequency is the average from 5 to 11 replicates. The standard errors of the means for the TI-112 day 14 and 21 frequencies were $\pm 0.22 \times 10^{-6}$ and $\pm 0.017 \times 10^{-6}$, respectively. The standard errors of the means for the TSCER2 day 14 and 21 frequencies were $\pm 4.77 \times 10^{-6}$ and $\pm 0.126 \times 10^{-6}$, respectively. The frequencies of untreated TI-112 and TSCER2 were $<0.06 \times 10^{-6}$ and $<0.1 \times 10^{-6}$, respectively.

[b] The estimated frequencies of convertant classes No-CO, CO-No-LOH, and CO-LOH-A are calculated by multiplication of the total frequency on day 14 by the percentage that each class represents within each collection of normal-growth convertants. Convertant classification is determined by haplotype linkage analysis.

[c] CO-LOH-B convertants are slow growing (see Materials and Methods) and are scored as late arising on day 21 and verified by the determination of doubling time.

[d] The overall crossover frequency represents the sum of the three crossover categories (CO-No-LOH, CO-LOH-A, and CO-LOH-B).

CO-LOH-A convertants frequently contain two independent cosegregated I-SceI-induced conversion tracts. The I-SceI site on *tk* allele A (Fig. 1) is expected to be lost during gene conversion, since extensive heterology is usually removed from the invading ends at the site of a recombinogenic break. However, cosegregation of a second, noncrossover copy of *tk* allele A in the CO-LOH-A class of convertants (Fig. 2) should result in the recovery of an intact I-SceI site unless this I-SceI site is also cut. Of 19 CO-LOH-A convertants (12 TSCER2 and 7 TI-112), only 1 (Fig. 5p) retained an I-SceI site, whereas 18 other CO-LOH-A convertants from TI-112 (Fig. 5q to t) and TSCER2 (Fig. 6f to n) had lost the I-SceI site on the noncrossover allele. These results indicate that the I-SceI site on the cosegregating chromosome is often cut at some point in the process.

HLA provides a methodology to directly determine the status of the I-SceI site on the noncrossover allele as well as to map a second, independent conversion tract that may result from cleavage of this site (Fig. 7). Selectable CO-LOH-A convertants can be wild type on the crossover allele or the noncrossover allele, which can be discriminated by separate HLA outcomes (Fig. 7, classes 2 and 3); class 4, in which convertants are wild type on both alleles, can be distinguished during the initial genotyping of the parental convertant. HLA would also

TABLE 2. Frequent recovery of long conversion tracts without selective pressure: summary of all 32 tract lengths in 16 CO-LOH-A clones

Cell line and tract length	No. of tracts					
	Unconstrained[a]			Constrained[b]		
	Noncrossover allele[c]	Crossover allele[d]	Total	Noncrossover allele	Crossover allele	Total
TI-112, short	4	0	4	0	0	0
TSCER2, short	2	2	4	6	2	8
TI-112, long	1	1	2	1	5	6
TSCER2, long	2	6	8	0	0	0
Total	9	9	18	7	7	14
Fraction of long tracts[e]	3/9	7/9	10/18	NA[f]	NA	NA

[a] An unconstrained conversion tract is one occurring on a *tk* allele that was not required for growth in CHAT. This allele can be tk^+ or tk^-.
[b] A constrained conversion tract is one occurring on a *tk* allele required for growth in CHAT. This allele is always tk^+.
[c] A noncrossover allele is defined here as the allele which segregated into a CO-LOH-A convertant and shows a parental arrangement for flanking microsatellite markers. This allele is often also recombined due to a second DSB-induced recombination event.
[d] A crossover allele is defined here as the allele which segregated into a CO-LOH-A convertant with rearranged flanking markers.
[e] Long tracts are those which minimally encompass the exon 4 FS site. In some cases these tracts encompass every marker within the *tk* locus, representing a minimum tract length of 12.1 kb. All other tracts that do not meet these criteria are classified as short.
[f] NA, not applicable. A tract length comparison is not meaningful, since constrained TSCER2 tracts are necessarily short and constrained TI-112 tracts are necessarily long.

permit the identification of nonrecombinational DSB repair (DSBR) products. However, in all cases the I-SceI insert was lost without any deletion of flanking sequences, indicating that the cosegregating DSBR product was always a gene conversion rather than a small intragenic deletion. Additionally, in all but three cases (Fig. 5q) additional *tk* polymorphisms were coconverted, thus further confirming the classification of these cosegregating alleles as recombinational products.

Unconstrained gene conversion tracts are often long. Since only one of the two alleles must be wild type for a convertant to be selected as CHAT resistant (Fig. 7), it was possible to recover and characterize cosegregated conversion tracts which were not constrained by the requirements of selection. Two separate conversion tracts were fully characterized in 16 CO-LOH-A clones derived from either TSCER2 or TI-112 (Table 2). In 14 convertants (Fig. 5q to t and 6f, g, and j to m), one of the two *tk* alleles is wild type and therefore necessary for growth in selective conditions; the conversion tract on the cosegregating allele, which retains an inactivating mutation, was thus unconstrained. Two cases (Fig. 6 h and i) involve cosegregating wild-type alleles. Both conversion tracts in each of these two cases are considered unconstrained for the purposes of this analysis.

This system was used to test the hypothesis that short conversion tracts would predominate when selection constraints were absent. Thus, the data (Table 2) are organized primarily by whether a tract was constrained by selection and its length; "long tracts" were defined as 7.0 kb or longer. Surprisingly, 10/18 unconstrained tracts were classified as long (Table 2), indicating that long tracts are common when recoverable. The long, unconstrained conversion tracts were recovered on both crossover and noncrossover alleles. Constrained tracts in both TI-112 and TSCER2 conform to expectations regarding length (Table 2) and complexity (Fig. 5q to t and 6f, g, and j to m).

Length of intragenic conversion tracts in TI-112. In addition to the unambiguous identification of crossovers associated with convertants, HLA permits the detailed analysis of polymorphic markers within the intragenic conversion tract, enabling the compilation of information regarding the length and complexity of the tracts. This system is not restricted to analysis of tracts on only the cut chromosome; tracts occurring on the donor chromosome are also distinguishable. A full representation of both tracts for all TI-112 clones (Fig. 5) and a summary of the distribution of conversion tract lengths from TI-112 convertants (Fig. 4A) are provided. In the summary, for simplicity, only one tract is presented for each clone. In some convertants (Fig. 5n), the length of the conversion tract is inferred from the location of the crossover relative to the DSB site, since intervening markers remain unaltered. In each case, the longest tract is shown, in order to demonstrate the frequent association between long tracts and crossover. CO-LOH-A clones are an exception, since only one of the tracts is directly associated with the crossover, whereas the other tract occurred independently of the crossover and cosegregated into the convertant. Thus, the crossover-associated tract was selected for display in the summary analysis (Fig. 4).

In TI-112, conversion tracts were all long (Fig. 4A) except in the case of some unconstrained tracts (Table 2; Fig. 5q and r). All remaining conversion tracts were a minimum of 7.0 kb long and as long as 12.1 kb. These are minimal estimates based on the position of the last known marker encompassed within the conversion tract. A large fraction (19/46; 41%) were observed to extend bidirectionally from the I-SceI site, and these occurred in both crossover and noncrossover clones (Fig. 4A).

Complexity of conversion tracts in TI-112. In cell line TI-112, only long and complex conversion tracts can be selected (Fig. 1B), although some unconstrained conversion tracts can also be recovered (Table 2). Selectable complex conversion tracts include a long and discontinuous conversion of the marker linked to the I-SceI site, 11.2 kb away, skipping the intervening exon 4 marker (Fig. 5a to f, k to m, o, s, u, and v). The second type is also long, with conversion of both the recipient I-SceI site and the donor exon 4 FS 7 kb from the cut site (Fig. 5g to i and p to r). A third type is a switch in linkage of either inactivating mutation, which can restore a wild-type *tk* allele on either chromosome (Fig. 5j, n, and t). The type of tract observed in any particular case is determined by whether the recombined A chromosome, the recombined B chromo-

TABLE 3. Most TI-112 recombinants involve discontinuous conversion of exon 1

Convertant category	No. of convertants[a]		
	Total	Co-No-LOH	No-CO
Opposite conversion of exon 4	4	0	4
Discontinuous conversion of exon 1 and switch of exon 4	4	2	2
Discontinuous conversion of exon 1	18	3	15
Switch of exon 1	4	3	1
Total	30	8	22

[a] A comparison of observed conversion categories is limited here to the No-CO and CO-No-LOH classes, since they can show any of the listed convertant categories. This is in contrast to both CO-LOH classes, which are restricted in showing different conversion categories due to the mitotic segregation which produced them. There is a statistically significant preference for conversion of the more distant exon 1 marker over conversion of the more DSB-proximal exon 4 FS on the template allele, compared to a null hypothesis that the two categories would be recovered with equal frequency (Fisher's exact test, $P = 0.01$).

TABLE 4. Alteration of markers on the donor chromosome supports a model of a common recombinational intermediate for crossovers and noncrossovers

Marker	No. of TI-112 convertants with altered donor chromosome markers[a]		
	NO-CO	CO-No-LOH	Total
Exon 7 FS	2	1	3
Exon 4 FS	4	2	6
Exon 1 TS	1	3	4
Exon 7 and exon 4	2	0	2
Fraction	9/22 (0.41)	6/8 (0.75)	15/30 (0.5)[b]

[a] Recoverable No-CO or CO-No-LOH convertants can show marker changes on the uncut donor chromosome but are not required to do so by selection constraints. On the other hand, CO-LOH-B convertants do not retain the uncut homologous chromosome due to the mitotic segregation that generated these clones. Similarly, CO-LOH-A convertants are forced to show marker transfer to produce a selectable event. Therefore, all CO-LOH convertants are excluded from this analysis.

[b] The fractions of convertants that show one or more markers with information transfer to the donor chromosome for No-CO and CO-No-LOH convertants are not statistically different (Fisher's exact test, $P = 0.21$).

some, or both recombined chromosomes segregated into the convertant.

By definition, only one of the two crossed-over chromosomes has segregated into a CO-LOH clone. This necessarily constrains conversion tract types in the CO-LOH-A and CO-LOH-B categories, although the selectable tracts are all complex. CO-LOH-B convertants are produced when the crossed-over A chromosome cosegregates with the non-crossed-over B chromosome (Fig. 2), which always showed the expected nonrecombinant parental haplotype (Fig. 5u to w). Therefore, by necessity all nine CO-LOH-B convertants show discontinuous conversion of the inactivating exon 1 TS on the A chromosome (Fig. 5u to w). Conversely, CO-LOH-A convertants are cosegregation products of the crossed-over B chromosome and the non-crossed-over A chromosome (Fig. 2). Therefore, with one exception (Table 2), selected CO-LOH-A tracts show opposite-direction conversion of the exon 4-inactivating FS on the B chromosome (Fig. 5p to t). Although the aforementioned CO-LOH tracts appear to be donor chromosome gene conversions, a crossover-associated linkage switch could produce the same outcome. The ability to distinguish these possibilities requires that both recombining chromosomes are available to be characterized, which is precluded by the segregation patterns in CO-LOH convertants (Fig. 2).

Both recombining chromosomes are cosegregated in CO-No-LOH convertants, by definition (Fig. 2). HLA is able to clearly identify this category of convertants, since the crossed-over flanking markers identify the presence of reciprocally recombined chromosomes in the parental convertant (Fig. 3). Analysis of the eight CO-No-LOH convertants recovered from TI-112 demonstrated that five were discontinuous conversions and the remaining three had undergone a crossover that included a function-restoring linkage switch of exon 1 (Fig. 5k to o; Table 3). On the other hand, while half of the 22 No-CO convertants (Fig. 5a to j; Table 3) will theoretically contain recombining chromosomes, they cannot be individually distinguished from nonrecombining cosegregants by flanking marker analysis. However, 17 of these No-CO convertants appear to have undergone conversion of exon 1 (Fig. 5a to f), whereas only 1 (Fig. 5j) showed a linkage switch that was localized to the marker in exon 1. This strong pattern suggests that among recoverable No-CO convertants, exon 1 is much more likely to have undergone a conversion than a localized switch, although we cannot rigorously confirm that conclusion for each individual case as we can for each CO-No-LOH convertant. The remaining four No-CO convertants (Fig. 5g to i; Table 3) showed an opposite conversion of the exon 4 FS. However, other No-CO convertants exhibited a localized linkage switch of exon 4 together with discontinuous conversion of exon 1 (Table 3; Fig. 5e and f). These results indicate that localized linkage switching and opposite conversion of the exon 4 marker both occur, although here again individual cases cannot be rigorously confirmed. Overall, with No-CO and CO-No-LOH convertants considered together, there were 22 gene conversions of exon 1 and 4 gene conversions of exon 4 (Table 3). This difference is statistically significant (Fisher's exact test, $P = 0.01$), suggesting that there is a mechanistic bias in favor of long conversion tracts that discontinuously convert the exon 1 TS (22/30). The preference for discontinuous conversion of exon 1 does not appear to be attributable to selection factors, since opposite-direction conversion of exon 4 was recovered in multiple cases.

Despite the preference for gene conversion of exon 1 as the mechanism for producing a selectable *tk* allele, alterations to one or more markers on the donor chromosome were seen frequently among both CO-No-LOH and No-CO convertants (Table 4). Such alterations were seen among markers on both sides of the DSB; in two, donor alterations on both sides of the I-SceI cut site were observed within the same convertant (Fig. 5e and f). All donor chromosome alterations, whether due to donor allele gene conversion or linkage switching, are particularly significant since they are indicative of specific models for recombination which allow for these change to occur (see discussion). In total, 15/30 CO-No-LOH and No-CO convertants showed examples of opposite conversion or linkage switching within the conversion tract. The occurrences of these alterations within both categories were not significantly different from each other (Table 4; Fisher's exact test, $P = 0.21$),

suggesting that crossover and noncrossover convertants share a common recombination intermediate.

Crossovers are mostly associated with long tracts in TSCER2. The spectrum of conversion tract lengths is presented for 95 TSCER2 convertants (Fig. 4B). In TSCER2 short and continuous conversion tracts 98 bp in length are selectable. The only tracts not selectable are long tracts that coconverted the exon 4-inactivating FS mutation, As expected from selection constraints, most tracts (86/95) were classified as short (Fig. 4B). Among 81 No-CO convertants (Fig. 6a to d), all converted the nearby exon 5 TS polymorphism, and 42/81 of these tracts also involved coconversion of the exon 7 FS (Fig. 6b). Although complexities in TSCER2 conversion tracts were less common than in TI-112, they were observed in 6 of 95 convertants, including all 3 crossover categories. The complex tracts included two CO-LOH-A and one CO-No-LOH conversion tracts in which the exon 7 FS was transferred to the donor chromosome (Fig. 6e, l, and m). Additionally, a long and discontinuous conversion tract was observed in a CO-LOH-B convertant (Fig. 6o), as is required for this class of crossovers. Finally, two No-CO convertants that exhibited opposite-direction conversion of the exon 7 FS (Fig. 6c) also met our criteria for classification as complex.

Surprisingly, 7/95 long tracts encompassed the exon 4 FS (Fig. 4B), despite our expectation that this site could not be included within selectable conversion tracts. These seven long tracts included the single discontinuous CO-LOH-B convertant (Fig. 6o) and six crossover-associated tracts from CO-LOH-A convertants (Fig. 6j to m). The six CO-LOH-A tracts were unconstrained (Table 2) and were recoverable only when cosegregating with an independent, selectable conversion tract into a CO-LOH-A recombinant. A further surprise is that long unconstrained tracts occurred in at least half of TSCER2 crossovers; the remaining 5/12 tracts were short CO-No-LOH and CO-LOH-A tracts. Since crossover-associated tracts of any length were recoverable in TSCER2, the high fraction of long tracts in these 12 convertants suggests that long tracts are common among crossovers. This observation is consistent with other lines of evidence, as discussed above (Table 1), that suggest a significant relationship between tract length and the occurrence of crossover.

Rare recombinants retain I-SceI sequence linked to a converted marker. Three convertants were recovered which defied expectations that the I-SceI site should always be converted when linked to the conversion of adjacent markers. In two of these three convertants (Fig. 5o and 6d) the I-SceI insert was partially deleted. Both cases are consistent with end-joining repair of a DSB. In addition, one CO-LOH-B clone retains a complete I-SceI insert on the chromosome which is also crossed over (Fig. 5w). As a group these three convertants could represent spontaneous recombinants, which may have also been cut and repaired by nonhomologous end joining within the same clone. Alternatively, these events could be attributable to triparental recombination involving both a sister chromatid and a homologous chromosome (see Discussion).

DISCUSSION

We report here the first extensive analysis of DSB-induced interchromosomal crossover in mammalian cells and descriptions of associated gene conversion tracts. This investigation was enabled by the development of an HLA methodology that provided an unambiguous demonstration of crossover as well as analysis of internal details of conversion tracts. The results demonstrate that crossovers are more frequent than anticipated, that conversion tracts in human cells are often many kilobases long and strongly associated with crossovers, and that long tracts are sometimes associated with internal complexities suggestive of recombination involving a double Holliday junction intermediate. We also report the first characterization of unselected interchromosomal conversion tracts from mammalian cells.

LOH is the product of crossover. Homozygosity of multiple linked chromosomal loci that is not due to mitotic nondisjunction has been commonly used in mammalian cells as an indication of crossover (60, 91). However, since the associated gene conversions and alternate segregation products cannot be observed, the possibility that other, noncrossover mechanisms could explain observations of LOH has remained. We have reported here interallelic crossovers with and without LOH, as expected for alternative segregation of crossover chromatids in postreplicative cells. I-SceI-induced crossovers were always associated with conversion within the gene (Fig. 5 and 6) and often produced homozygosis of the *tk*-flanking microsatellite polymorphism linked to the DSB (Fig. 5p to t and 6f to n). This is not what would be expected for the products of an alternate mechanism for extensive homozygosity known as break-induced replication (BIR) (54). Those products that did show homozygosity for the flanking markers on the donor chromosome (CO-LOH-B) were also discontinuous from the site of the DSB (Fig. 5u to w and 6o); again, this is not what has been observed for BIR (45). In this pathway, a single broken end invades and initiates replication of whole chromosomal arms while the terminal fragment produced by the break is lost; BIR thus results in homozygosity for markers on the unbroken chromosome. Therefore, the results presented here confirm that LOH may commonly result from mitotic crossover. This does not exclude the possibility that I-SceI-induced DSBs could also produce the types of terminal multilocus LOH seen in tumor cells (15) by a BIR mechanism, since these would not be selectable outcomes in TSCER2 and TI-112.

Crossovers are associated with long conversion tracts. Among the few previous studies of interchromosomal gene conversion tracts and crossover in mammalian cells (29, 71, 72, 80, 83), crossovers have been rarely if ever observed. Some authors have therefore hypothesized that crossovers are suppressed in mammalian cells (83). We report here, however, that 16% of convertants in TSCER2 were associated with a crossover (Table 1), indicating that crossovers can be associated with conversion in mammalian cells at a level comparable to that in *Saccharomyces cerevisiae* (54, 64). For *S. cerevisiae* it has also been reported that a minimum of 1.7 kb of homology was required to recover DSB-induced crossovers (39). Those authors further proposed that this length represents the minimal region necessary to form a stable double Holliday junction structure. An analysis of our results (Fig. 4) also suggests a strong association of long tracts and crossovers. We observed here that 7/12 TSCER2 crossovers were associated with conversion tracts that were minimally 7.0 kb in length (Fig. 4), which is consistent with expectations that tract length and

crossover would extend to mammalian recombination. These results are supported by observations of TI-112 (Fig. 4), in which long tracts are required for selection. Although there is no corresponding requirement for crossover, approximately half of long tracts in the TI-112 system are indeed associated with a crossover (Fig. 4). The results of our study may suggest that crossovers can occasionally occur in association with short conversion tracts (Fig. 4), which are necessarily defined by the inclusion of known polymorphic markers. However, in each case crossover-associated conversion tracts could extend significantly beyond the last polymorphism known to be included within the tract, which would then constitute a tract of at least several kilobases in length. The high fraction of multilocus LOH attributable to crossover in the forward mutant spectrum of TK6 lymphoblasts and their derivatives (47) is similar to that for other somatic cell types in vivo (33, 49, 61, 78, 92) and in vitro (19, 20, 43), suggesting that the crossovers observed in this study are not atypical.

Studies examining the crossover association of DSB-induced interchromosomal gene conversion in mammalian cells are quite limited. A strong relationship between conversion tract length and crossover might explain the absence of crossovers in systems that preclude or select against long conversion tracts. For instance, when homologous substrates were short, crossovers were unobserved (71). Only one other study has been performed to date that could potentially detect both CO-LOH and CO-No-LOH products in association with DSB-induced interallelic gene conversion. In this mouse embryonic stem (ES) cell study (83), crossovers were not observed and conversion tracts were overwhelmingly short; 158/162 were 1 kb long or less, and 145 of these were less than 0.3 kb in length (83). The reason that only a few long tract convertants were observed (83) may in part be due to the potential for coconversion of the closely placed (526 bp) inactivating mutation on the opposite allele. A similar marker configuration has been shown to significantly reduce the recovery of long tracts for interallelic gene conversion in yeast (64). In addition, the restriction fragment length polymorphism markers used for linkage analysis did not permit determination of crossover association for the few long conversion tracts that were recovered (83).

Long (3.2-kb) and one-sided gene conversion tracts were frequently observed in other ES cell studies involving short interchromosomal substrates (69) or a tandem repeat recombinational substrate designed to observe unequal sister chromatid recombination (42). Notably, long conversion tracts in these systems would necessarily extend into regions of nonhomology (42, 69) or through a region of interrupted homology (42). Restrictions on the formation of extensive heteroduplex DNA may thus account for the lack of crossovers in these investigations. Further insight might also be inferred from analysis of common tumor-associated chromosomal translocations, which map to the very long homologous regions (>10 kb to 400 kb) within the genomic features known as low-copy repeats and which are attributed to crossover (6, 8). In contrast translocations in somatic cells involving relatively short sequences such as *Alu* repeats are generated by single-strand annealing or nonhomologous end joining (22, 70) rather than crossover, and breakpoint analysis of many tumor-associated translocations supports these observations (93).

Recombination following endonuclease-induced sister chromatid breaks. The use of HLA enabled the observation that I-SceI sites from sister chromatids had each been cut and undergone separate conversion events (Fig. 7), at least in a subset of convertants. This would be expected to commonly occur in studies that utilize highly expressed endonucleases for generating DSBs, but it has rarely been possible to rigorously identify and characterize such events (42). Interestingly, 6/12 CO-LOH-A crossovers in TSCER2 (Fig. 6j to m) were selectable only due to the occurrence of a second conversion tract, since the crossover-associated conversion tract did not restore TK function (Fig. 7, class 3). Due to the configuration of the markers in the test locus, this pathway cannot lead to the recovery of CO-LOH-B or CO-No-LOH events. We therefore hypothesize that long continuous tracts are common but are recoverable only in the CO-LOH-A category, thus accounting for the bias in recovery of the CO-LOH-A category among TSCER2 crossovers (Table 1). It should be noted that CO-LOH-B tracts are all necessarily long and complex, suggesting that these occur less frequently than long and continuous tracts. These results also suggest that the TSCER2 system is efficiently scoring crossovers that occur, although there may still be an underestimate for nonfunctional crossover alleles which did not cosegregate with a separately converted allele that had been restored to function.

The higher recovery of crossovers in this study is unlikely to be attributable to the occurrence of two DSB, since other endonuclease-induced mammalian and yeast studies would have a similar circumstance. The difference here is the ability of HLA analysis to dissect out the independent conversion tracts arising from each break (Fig. 7). This analysis reveals no evidence that the occurrence of two breaks affected the nature of the resultant conversion tracts. In contrast, each tract generally appears to be independent of the other based on analysis of internal structure and length (Fig. 5 and 6). The likelihood of crossover association would also appear to be unaffected based on comparison of our results to those on endonuclease-induced recombination in other systems. For example, mammalian cell studies generally report few if any crossovers (42, 83), though the opportunity for two strand breaks is similar to the situation in the present investigation. In *Drosophila melanogaster*, the crossover fraction has surprisingly been reported to increase when the I-SceI endonuclease was expressed at a lower level (74).

A previous study of 38 I-SceI-induced TSCER2 convertants did not observe any crossovers as measured by multilocus LOH (37). This is in contrast to our observation that 12/95 (0.13) TSCER2 convertants could be classified as CO-LOH-A events (Fig. 4B). To understand the difference in these findings, it is important to appreciate that half of the CO-LOH-A convertants reported here required two conversion tracts to be selected (Fig. 6j to m). We hypothesize that the recovery of this group of crossovers in the earlier study (37) may be specifically diminished due to the utilization of an electroporation technology for transfection of I-SceI expression plasmid that was orders-of-magnitude less efficient (38; E. A. H. Neuwirth and A. J. Grosovsky, unpublished results). This efficiency difference may further be reflected in a 40-fold-higher conversion frequency (Table 1) compared to previous results (37). We thus suggest that the adjusted number of expected crossovers in

the previous collection of 38 I-SceI convertants would be (0.13)(38)/2 = 2.47. The failure to observe any crossovers could be attributable to the smaller size of the collection and statistical fluctuations in recovering an anticipated 2.5 crossovers.

Unconstrained gene conversion tracts are often long. Two conversion events within the same recombinant clone made it possible to analyze a conversion tract that was not restricted by the requirements of selection. Significantly, unconstrained tracts were often long, at least 7.0 kb, and included both crossover-associated and non-crossover-associated tracts (Table 2). The data reported here represent the first mammalian cell analysis of interchromosomal homologous recombinational repair tract length in a nonselective context and demonstrate that conversion tracts extend over a much longer region than generally reported with short homologous substrates (21, 23, 87). As discussed above, in a study of mouse ES cell interallelic recombination (83), tracts constrained by selection to be unidirectional were primarily very short. Locus design constraints in TSCER2 also exist, since in the absence of cosegregation with a wild-type allele, coconversion of the exon 4 FS 7 kb from the cut site precludes the selection of long, noncrossover convertants (Fig. 1; Table 4). However, the observation of long and unconstrained tracts among noncrossover conversion tracts (Table 2) suggests that a significant portion of the selectable conversion tract spectrum was actually longer than could be established here due to the distance between available polymorphic markers (Fig. 1; Table 4). Additionally, these findings suggest that long tracts that coconvert exon 4 would represent a significant component of all recombination that occurs, even if they are not represented in the collection of convertants.

Evidence for triparental recombination in mammalian cells. Several convertants (Fig. 5o and w and 6d) which retain all or part of the I-SceI site on the recombined chromosome were recovered. This could suggest the recovery of spontaneous convertants in the collection, although this seems unlikely due to frequency considerations. The background interchromosomal conversion frequency in a closely related cell line is 3×10^{-8} (67; Neuwirth and Grosovsky, unpublished data), whereas the I-SceI-induced conversion frequencies are $4{,}000 \times 10^{-8}$ in TSCER2 and 154×10^{-8} in TI-112 (Fig. 6). An alternative explanation is that these convertants are I-SceI induced and are products of a previously described triparental recombination mechanism (27). Under this model, the ends of one break separately invade the homolog and the sister chromatid. Recombination with the homolog eliminates the I-SceI insert but allows conversion of adjacent markers, whereas recombination with the sister restores the I-SceI site on the broken chromatid. The small set of convertants that retain the I-SceI site on the recombined chromosome are consistent with the predictions of this model and thus may be considered evidence for the occurrence of this pathway in mammalian cells.

Potential mechanisms for long tract recombination. The only recombinational model that can explain the full spectrum of observed convertant clones is the DSBR model for recombination (84, 86). Other models that allow for crossovers, such as a migrating D-loop model (24), are one sided and do not allow for convertants with complex alterations such as bidirectional tracts with donor allele alterations (see, for instance, Fig. 5c to f). There are several processes within the DSBR model which might be responsible for the very long tracts observed in TI-112 and TSCER2 convertants. Donor allele conversion in interallelic yeast systems was previously reported as evidence of Holliday junction branch migration and mismatch repair within symmetric heteroduplex DNA (57, 64) and similarly could explain the complex tract structures observed in TI-112 (Fig. 8a1; Tables 3 and 4) and TSCER2 (Fig. 6). In support of this model, symmetric heteroduplex DNA in mammalian cells has been reported in analysis of targeted gene insertion (9), occurring within crossover-associated conversion tracts of as long as 6 kb. If long symmetric heteroduplexes formed in TI-112, we would expect opposite-allele conversion of exon 4, which is relatively close to the I-SceI site, to occur more frequently than discontinuous conversion involving the more distant exon 1 (Fig. 1). However, we found that discontinuous conversion of exon 1 was four- to fivefold more common than donor allele conversion of exon 4 (Table 3).

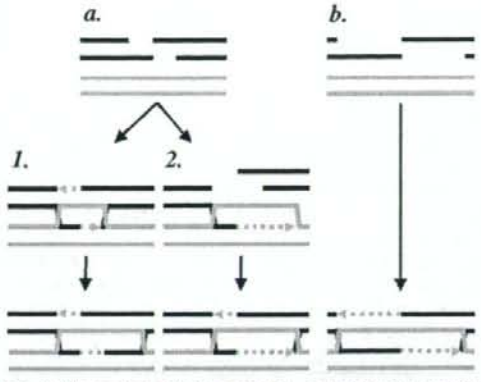

FIG. 8. Mechanisms for long-distance recombination associated with crossovers. Variations on the DSBR model (84, 86) for recombination are shown. (a) Resection of the 5′ ends is not extensive. 1, Following strand invasion and repair synthesis, Holliday junctions form, branch migrate, and produce a long region of symmetric heteroduplex DNA. 2, Repair synthesis continues beyond the region of limited resection, producing a long displacement loop. Additional resection allows the D loop to form a long asymmetric heteroduplex on the other side of the break. This also allows Holliday junctions to form. (b) Initial strand resection is very extensive. Holliday junction formation requires a region of repair synthesis as long as the region of resection.

The predominance of exon 1 conversion among TI-112 convertants can alternatively be explained by an asymmetric heteroduplex DNA model if combined with D-loop displacement and pairing (Fig. 8). Long repair synthesis could drive the formation of a long asymmetric heteroduplex (10, 55), although repair synthesis and resection must be equally long for Holliday junctions to form (66). The necessary resection could most simply occur prior to strand invasion (Fig. 8b), although it has been suggested (55) that resection could be completed following strand invasion (Fig. 8a). Either way, generation of a selectable outcome in TI-112 by this model would require conversion of exon 1 without coconversion of exon 4 (Fig. 1), resulting in the observation of a "discontinuous" conversion tract. The action of mismatch repair on the heteroduplex can

produce the necessary configuration for selection if heteroduplex pairings in exon 4 and exon 1 are separately resolved. Since mismatches have been reported to be independently repaired when separated by only hundreds of bases (59), the 4.3-kb interval between the exon 4 and exon 1 polymorphisms (Fig. 1) seems sufficiently long to allow for independent resolution.

Conclusions. The results presented here suggest that long gene conversion tracts are surprisingly frequent. Furthermore, crossovers were strongly associated with long tracts, even though shorter crossover-associated tracts were just as easily observable. Many of the long tracts observed here were also complex, which could potentially be an additional factor stimulating crossover. It has been suggested (95) that crossovers are suppressed in order to avoid the mutagenic potential associated with LOH or translocations and that crossover may be suppressed in human cells to a greater extent than in yeast (83). However, the findings presented here suggest that yeast and humans may be more comparable than previously known with respect to the regulation of crossover.

ACKNOWLEDGMENTS

The I-SceI expression vector pCBASce was kindly provided to M. Honma by M. Jasin.

This work was supported by grant NAG2-1638 from the National Air and Space Administration. E.A.H.N. was also supported by a grant from the University of California, Toxic Substances Research and Teaching Program.

REFERENCES

1. **Aguilera, A., and H. L. Klein.** 1989. Yeast intrachromosomal recombination: long gene conversion tracts are preferentially associated with reciprocal exchange and require the RAD1 and RAD3 gene products. Genetics **123:** 683–694.
2. **Ahn, B. Y., and D. M. Livingston.** 1986. Mitotic gene conversion lengths, coconversion patterns, and the incidence of reciprocal recombination in a *Saccharomyces cerevisiae* plasmid system. Mol. Cell. Biol. **6:**3685–3693.
3. **Aldosari, N., B. K. Rasheed, R. E. McLendon, H. S. Friedman, D. D. Bigner, and S. H. Bigner.** 2000. Characterization of chromosome 17 abnormalities in medulloblastomas. Acta Neuropathol. (Berlin) **99:**345–351.
4. **Amundson, S. A., and H. L. Liber.** 1991. A comparison of induced mutation at homologous alleles of the tk locus in human cells. Mutat. Res. **247:**19–27.
5. **Amundson, S. A., and H. L. Liber.** 1992. A comparison of induced mutation at homologous alleles of the tk locus in human cells. II. Molecular analysis of mutants. Mutat. Res. **267:**89–95.
6. **Barbouti, A., P. Stankiewicz, C. Nusbaum, C. Cuomo, A. Cook, M. Hoglund, B. Johansson, A. Hagemeijer, S. S. Park, F. Mitelman, J. R. Lupski, and T. Fioretos.** 2004. The breakpoint region of the most common isochromosome, i(17q), in human neoplasia is characterized by a complex genomic architecture with large, palindromic, low-copy repeats. Am. J. Hum Genet. **74:**1–10.
7. **Benjamin, M. B., and J. B. Little.** 1992. X rays induce interallelic homologous recombination at the human thymidine kinase gene. Mol. Cell. Biol. **12:**2730–2738.
8. **Bi, W., S. S. Park, C. J. Shaw, M. A. Withers, P. I. Patel, and J. R. Lupski.** 2003. Reciprocal crossovers and a positional preference for strand exchange in recombination events resulting in deletion or duplication of chromosome 17p11.2. Am. J. Hum. Genet. **73:**1302–1315.
9. **Birmingham, E. C., S. A. Lee, R. D. McCulloch, and M. D. Baker.** 2004. Testing predictions of the double-strand break repair model relating to crossing over in mammalian cells. Genetics **168:**1539–1555.
10. **Blanton, H. L., S. J. Radford, S. McMahan, H. M. Kearney, J. G. Ibrahim, and J. Sekelsky.** 2005. REC, Drosophila MCM8, drives formation of meiotic crossovers. PLoS Genet. **1:**e40.
11. **Boley, S. E., E. E. Anderson, J. E. French, L. A. Donehower, D. B. Walker, and L. Recio.** 2000. Loss of p53 in benzene-induced thymic lymphomas in p53+/− mice: evidence of chromosomal recombination. Cancer Res. **60:** 2831–2835.
12. **Bollag, R. J., and R. M. Liskay.** 1988. Conservative intrachromosomal recombination between inverted repeats in mouse cells: association between reciprocal exchange and gene conversion. Genetics **119:**161–169.
13. **Bollag, R. J., A. S. Waldman, and R. M. Liskay.** 1989. Homologous recombination in mammalian cells. Annu. Rev. Genet. **23:**199–225.
14. **Bradshaw, H. D., Jr., and P. L. Deininger.** 1984. Human thymidine kinase gene: molecular cloning and nucleotide sequence of a cDNA expressible in mammalian cells. Mol. Cell. Biol. **4:**2316–2320.
15. **Cavenee, W. K., T. P. Dryja, R. A. Phillips, W. F. Benedict, R. Godbout, B. L. Gallie, A. L. Murphree, L. C. Strong, and R. L. White.** 1983. Expression of recessive alleles by chromosomal mechanisms in retinoblastoma. Nature **305:**779–784.
16. **Clive, D.** 1973. Recent developments with the L5178Y TK heterozygote mutagen assay system. Environ. Health Perspect. **6:**119–125.
17. **Collins, L., and C. S. Newlon.** 1994. Meiosis-specific formation of joint DNA molecules containing sequences from homologous chromosomes. Cell **76:** 65–75.
18. **Cromie, G. A., and D. R. Leach.** 2000. Control of crossing over. Mol. Cell **6:**815–826.
19. **de Nooij-van Dalen, A. G., V. H. van Buuren-van Seggelen, A. Mulder, K. Gelsthorpe, J. Cole, P. H. Lohman, and M. Giphart-Gassler.** 1997. Isolation and molecular characterization of spontaneous mutants of lymphoblastoid cells with extended loss of heterozygosity. Mutat. Res. **374:**51–62.
20. **Dobo, K. L., C. R. Giver, D. A. Eastmond, H. S. Rumbos, and A. J. Grosovsky.** 1995. Extensive loss of heterozygosity accounts for differential mutation rate on chromosome 17q in human lymphoblasts. Mutagenesis **10:**53–58.
21. **Elliott, B., and M. Jasin.** 2001. Repair of double-strand breaks by homologous recombination in mismatch repair-defective mammalian cells. Mol. Cell. Biol. **21:**2671–2682.
22. **Elliott, B., C. Richardson, and M. Jasin.** 2005. Chromosomal translocation mechanisms at intronic alu elements in mammalian cells. Mol. Cell **17:**885–894.
23. **Elliott, B., C. Richardson, J. Winderbaum, J. A. Nickoloff, and M. Jasin.** 1998. Gene conversion tracts from double-strand break repair in mammalian cells. Mol. Cell. Biol. **18:**93–101.
24. **Ferguson, D. O., and W. K. Holloman.** 1996. Recombinational repair of gaps in DNA is asymmetric in Ustilago maydis and can be explained by a migrating D-loop model. Proc. Natl. Acad. Sci. USA **93:**5419–5424.
25. **Fitzgibbon, J., L. L. Smith, M. Raghavan, M. L. Smith, S. Debernardi, S. Skoulakis, D. Lillington, T. A. Lister, and B. D. Young.** 2005. Association between acquired uniparental disomy and homozygous gene mutation in acute myeloid leukemias. Cancer Res. **65:**9152–9154.
26. **Flemington, E., H. D. Bradshaw, Jr., V. Traina-Dorge, V. Slagel, and P. L. Deininger.** 1987. Sequence, structure and promoter characterization of the human thymidine kinase gene. Gene **52:**267–277.
27. **Gilbertson, L. A., and F. W. Stahl.** 1996. A test of the double-strand break repair model for meiotic recombination in Saccharomyces cerevisiae. Genetics **144:**27–41.
28. **Giver, C. R., and A. J. Grosovsky.** 2000. Radiation specific patterns of loss of heterozygosity on chromosome 17q. Mutat. Res. **450:**201–209.
29. **Godwin, A. R., R. J. Bollag, D. M. Christie, and R. M. Liskay.** 1994. Spontaneous and restriction enzyme-induced chromosomal recombination in mammalian cells. Proc. Natl. Acad. Sci. USA **91:**12554–12558.
30. **Godwin, A. R., and R. M. Liskay.** 1994. The effects of insertions on mammalian intrachromosomal recombination. Genetics **136:**607–617.
31. **Grist, S. A., M. McCarron, A. Kutlaca, D. R. Turner, and A. A. Morley.** 1992. In vivo human somatic mutation: frequency and spectrum with age. Mutat. Res. **266:**189–196.
32. **Grosovsky, A. J., B. N. Walter, and C. R. Giver.** 1993. DNA-sequence specificity of mutations at the human thymidine kinase locus. Mutat. Res. **289:**231–243.
33. **Gupta, P. K., A. Sahota, S. A. Boyadjiev, S. Bye, C. Shao, J. P. O'Neill, T. C. Hunter, R. J. Albertini, P. J. Stambrook, and J. A. Tischfield.** 1997. High frequency in vivo loss of heterozygosity is primarily a consequence of mitotic recombination. Cancer Res **57:**1188–1193.
34. **Hagstrom, S. A., and T. P. Dryja.** 1999. Mitotic recombination map of 13cen-13q14 derived from an investigation of loss of heterozygosity in retinoblastomas. Proc. Natl. Acad. Sci. USA **96:**2952–2957.
35. **Haigis, K. M., J. G. Caya, M. Reichelderfer, and W. F. Dove.** 2002. Intestinal adenomas can develop with a stable karyotype and stable microsatellites. Proc. Natl. Acad. Sci. USA **99:**8927–8931.
36. **Holliday, R.** 1964. A mechanism for gene conversion in fungi. Genet. Res. **5:**282–304.
37. **Honma, M., M. Izumi, M. Sakuraba, S. Tadokoro, H. Sakamoto, W. Wang, F. Yatagai, and M. Hayashi.** 2003. Deletion, rearrangement, and gene conversion; genetic consequences of chromosomal double-strand breaks in human cells. Environ. Mol. Mutagen. **42:**288–298.
38. **Honma, M., M. Sakuraba, T. Koizumi, Y. Takashima, H. Sakamoto, and M. Hayashi.** 2007. Non-homologous end-joining for repairing I-SceI-induced DNA double strand breaks in human cells. DNA Repair (Amsterdam) **6:**781–788.
39. **Inbar, O., B. Liefshitz, G. Bitan, and M. Kupiec.** 2000. The relationship between homology length and crossing over during the repair of a broken chromosome. J. Biol. Chem. **275:**30833–30838.
40. **James, C. D., E. Carlbom, M. Nordenskjold, V. P. Collins, and W. K.**